Specific modulation of the root immune system by a community of commensal bacteria

Paulo J. P. L. Teixeira[a,b,1,2], Nicholas R. Colaianni[a,b,c,2], Theresa F. Law[a,b,2], Jonathan M. Conway[a,b,2], Sarah Gilbert[a,b], Haofan Li[d,3], Isai Salas-González[a,b,c], Darshana Panda[a], Nicole M. Del Risco[a], Omri M. Finkel[a,b,4], Gabriel Castrillo[a,b,5], Piotr Mieczkowski[e,f], Corbin D. Jones[b,c,e,f,g], and Jeffery L. Dangl[a,b,c,g,h,6]

[a]HHMI, University of North Carolina at Chapel Hill, Chapel Hill, NC 27599; [b]Department of Biology, University of North Carolina at Chapel Hill, Chapel Hill, NC 27599; [c]Curriculum in Bioinformatics and Computational Biology, University of North Carolina at Chapel Hill, Chapel Hill, NC 27599; [d]Department of Biology, Kenyon College, Gambier, OH 43022; [e]Department of Genetics, University of North Carolina at Chapel Hill, Chapel Hill, NC 27599; [f]Lineberger Comprehensive Cancer Center, University of North Carolina at Chapel Hill, Chapel Hill, NC 27599; [g]Curriculum in Genetics and Molecular Biology, University of North Carolina at Chapel Hill, Chapel Hill, NC 27599; and [h]Department of Microbiology and Immunology, University of North Carolina at Chapel Hill, Chapel Hill, NC 27599

Contributed by Jeffery L. Dangl, March 8, 2021 (sent for review January 19, 2021; reviewed by Sheng Yang He and Venkatesan Sundaresan)

Plants have an innate immune system to fight off potential invaders that is based on the perception of nonself or modified-self molecules. Microbe-associated molecular patterns (MAMPs) are evolutionarily conserved microbial molecules whose extracellular detection by specific cell surface receptors initiates an array of biochemical responses collectively known as MAMP-triggered immunity (MTI). Well-characterized MAMPs include chitin, peptidoglycan, and flg22, a 22-amino acid epitope found in the major building block of the bacterial flagellum, FliC. The importance of MAMP detection by the plant immune system is underscored by the large diversity of strategies used by pathogens to interfere with MTI and that failure to do so is often associated with loss of virulence. Yet, whether or how MTI functions beyond pathogenic interactions is not well understood. Here we demonstrate that a community of root commensal bacteria modulates a specific and evolutionarily conserved sector of the *Arabidopsis* immune system. We identify a set of robust, taxonomically diverse MTI suppressor strains that are efficient root colonizers and, notably, can enhance the colonization capacity of other tested commensal bacteria. We highlight the importance of extracellular strategies for MTI suppression by showing that the type 2, not the type 3, secretion system is required for the immunomodulatory activity of one robust MTI suppressor. Our findings reveal that root colonization by commensals is controlled by MTI, which, in turn, can be selectively modulated by specific members of a representative bacterial root microbiota.

plant immunity | root microbiome | MAMP | SynCom | flg22

Plants are inhabited by hundreds of species of commensals, many of which have beneficial effects on the host (1). These microbes often express the same immunogenic microbe-associated molecular patterns (MAMPs) that are found in pathogens, highlighting their potential to trigger immune responses in their hosts (2–4). How plants mount effective defenses against pathogens while allowing the colonization of commensals remains a mystery. Plant-associated microbial communities are much less diverse than those of the surrounding environment (1), indicating that the host exerts selection pressure over their microbiota and that some microbes are better adapted to colonize plant tissues than others. While multiple environmental and genetic factors likely orchestrate microbiota assembly and structure, recent research indicates that the plant immune system operates as a major gatekeeper. *Arabidopsis thaliana* plants (hereafter *Arabidopsis*) compromised in the signaling of the defense phytohormones salicylic acid and jasmonic acid harbor altered microbiota (5, 6). Similarly, mutants impaired in MAMP-triggered immunity (MTI) and in the MIN7-vesicle trafficking pathway carry altered endophytic phyllosphere microbiota and display leaf-tissue damage associated with dysbiosis under conditions of high humidity (7). Recent evidence demonstrates that perception of flg22 is usually low in most root cells, but upregulated following tissue wounding associated with infection and potentially colonization (8, 9).

Significance

In natural environments, plants establish intimate interactions with a wide diversity of microbes. It is unknown, however, how microbiota composed of commensal bacteria colonize roots in the face of a sophisticated plant immune system that evolved to recognize microbial-associated molecular patterns. We investigate the interaction between plant immune system function and the root microbiota. We report that root-associated commensal bacteria actively suppress the host immune response in the context of a community. Suppressors and nonsuppressors co-occur in the root microbiome and the presence of the former can enhance the colonization ability of the latter. We highlight the role of a specific sector of the plant immune system and its suppression in gating microbial access to the roots.

Author Contributions: J.L.D. supervised the project; P.J.P.L.T. and J.L.D. conceptualized the project; P.J.P.L.T., N.R.C., T.F.L., J.M.C., S.G., and J.L.D. designed experiments; T.F.L. oversaw SynComs and mono-associations experiments; P.J.P.L.T., T.F.L., O.M.F., and G.C. performed experiments to evaluate plant transcriptomes through RNA-seq; P.J.P.L.T. prepared RNA-seq libraries; P.M. advised and oversaw the sequencing of RNA-seq libraries; P.J.P.L.T. and N.R.C. processed and analyzed RNA-seq data, with input from C.D.J.; P.J.P.L.T., T.F.L., and H.L. measured root lengths; T.F.L. and S.G. performed experiment and prepared libraries for 16S amplicon sequencing; N.R.C. and I.S.-G. analyzed 16S data; T.F.L. and S.G. measured bacterial colonization of plant roots; P.J.P.L.T. and H.L. evaluated the acute flg22 response using GUS reporter lines; N.R.C. performed statistical analyses with input from C.D.J. and I.S.-G.; J.M.C., D.P., and N.M.D.R designed and performed bacterial genetics analyses, including the transposon library screening; and P.J.P.L.T. wrote the manuscript with text contributions and editing input from N.R.C., T.F.L., J.M.C., S.G., and J.L.D.

Reviewers: S.Y.H., Duke University; and V.S., University of California, Davis.

Competing interest statement: J.L.D. is a cofounder of, and shareholder in, AgBiome LLC, a corporation whose goal is to use plant-associated microbes to improve plant productivity.

[1]Present address: Department of Biology, "Luiz de Queiroz" College of Agriculture, University of São Paulo, 13418-900 São Paulo, Brazil.

[2]P.J.P.L.T., N.R.C., T.F.L., and J.M.C. contributed equally to this work.

[3]Present address: Biological & Biomedical Sciences, Yale School of Medicine, New Haven, CT 06510.

[4]Present address: Department of Plant and Environmental Sciences, Institute of Life Sciences, The Hebrew University of Jerusalem, 9190501 Jerusalem, Israel.

[5]Present address: Future Food Beacon of Excellence and the School of Biosciences, University of Nottingham, LE12 5RD Sutton Bonington, United Kingdom.

[6]To whom correspondence may be addressed. Email: dangl@email.unc.edu.

This article contains supporting information online at https://www.pnas.org/lookup/suppl/doi:10.1073/pnas.2100678118/-/DCSupplemental.

Published April 16, 2021.

The ability to suppress the host immune response is a hallmark of successful pathogens (10). In animals, both specific and redundant immunomodulatory effects have been defined for taxonomically diverse commensal gut bacteria (11). Likewise, plant-associated commensals have been shown to modulate MTI (12–19). Nevertheless, studies in plants have so far focused on single microbes and the specific immunomodulatory effects of different strains have not been integrated in the context of complex communities. Furthermore, the significance of immunomodulation for community assembly remains unexplored. In this work, we investigated how a community of root-associated commensal bacteria interacts with the *Arabidopsis* immune system. We verified that the ability to suppress MTI is common and taxonomically widespread among these commensals. High-throughput gene-expression analyses of plants colonized by synthetic communities (SynComs) or by single microbes led to the identification of a set of defense-related genes that were commonly manipulated by phylogenetically distinct suppressor strains, highlighting a sector of the plant immune system that may control plant colonization by the microbiota. Notably, suppressors could promote the growth of other nonsuppressor strains, indicating that certain microbes may benefit from co-occurring suppressor strains. Furthermore, a genetic screening revealed that the type 2 secretion system (T2SS) is required for the robust suppressor *Dyella japonica* MF79 to interfere with root MTI, while the type 3 secretion system (T3SS) was dispensable. Our results expand our understanding of how the plant immune system functions in roots colonized by commensals, underscoring the role of MTI and of its suppression in microbiota assembly.

Results

A Community of Root Commensals Suppresses MTI. To understand how MAMP-triggered immunity affects the composition of the root microbiome and whether root-associated bacteria can modulate this immune response in the context of a commensal community, we established a model system (*SI Appendix*, Fig. S1 *A–E*). Here, 7-d-old *Arabidopsis* seedlings were exposed for 12 d to 1 μM of the bacterial peptide MAMP flg22. Although MTI has been traditionally studied within minutes/hours of MAMP exposure (15, 20, 21), we validated that the continuous presence of flg22 in our system induces a defense-related transcriptional signature that is functionally overlapping with the one observed in "typical" systems (*SI Appendix*, Fig. S1*F*), indicating that flg22 signaling and immunogenicity persist for at least 12 d. Using this system, we concurrently inoculated plants with 1 μM flg22 or not and a 35-member bacterial synthetic community composed of a random consortium of *Arabidopsis* root commensals (SynCom35) (Dataset S1) that is phylogenetically representative of wild-soil root-associated microbiota (22). Interestingly, bacterial 16S profiles revealed only minor differences between the communities of bacteria colonizing flg22-treated roots and those colonizing untreated plants (Fig. 1*A*). Only two bacterial taxa had differential abundances in the roots of plants exposed to flg22 (*SI Appendix*, Fig. S1*G* and Dataset S2). Thus, overall community composition was not affected by the addition of the elicitor flg22, suggesting that SynCom35 interferes with the plant immune response to facilitate community assembly in the face of flg22-driven MTI.

To investigate whether SynCom35 interferes with the flg22-induced immune response in roots, we cultivated plants in axenic conditions, in the presence of SynCom35, or in the presence of heat-killed SynCom35 (2 h at 100 °C) (*SI Appendix*, Fig. S1 *C–E*). Roots exposed to flg22 for 12 d without any bacteria or in the presence of the heat-killed SynCom35 displayed a clear transcriptional reprogramming, with 492 and 523 genes responding to the elicitor, respectively (Fig. 1*B* and Dataset S3). The flg22-responsive genes from these control treatments were not only highly overlapping (Fig. 1*C*), but also showed highly correlated expression levels (Fig. 1*D*), demonstrating that the dead bacterial community does not interfere with the plant response to flg22. In contrast, only seven genes responded to flg22 in plants inoculated with the live SynCom35 (Fig. 1*B*), and no correlation was observed between this condition and the two other controls (Fig. 1 *C* and *D*). Indeed, SynCom35 triggered a unique transcriptional signature that persisted in the presence of flg22 (Fig. 1*E*). Hierarchical clustering revealed a set of 281 genes (39% of the total flg22-responsive genes) that were clearly activated by flg22 in the roots of control plants, but strongly suppressed when SynCom35 was also present (cluster SC1 in Fig. 1 *F* and *G*). Cluster SC1 is strongly enriched in immune-related genes (Fig. 1*H*), demonstrating that this bacterial commensal community possesses immunomodulatory activity.

WRKY transcription factors, which include master regulators of plant immunity (23), were overrepresented in cluster SC1 (P = 8.8E-6) (*SI Appendix*, Fig. S2 *A–E*), which contained seven of the eight *WRKY* genes that were up-regulated by flg22. Consistent with a suppressed WRKY regulatory network, cluster SC1 was also enriched in predicted targets of these transcription factors (*SI Appendix*, Fig. S2*F*). SynCom35 also suppressed the activation of genes encoding receptor-like kinases (RLKs) (*SI Appendix*, Fig. S2*G*), including the MTI marker *FRK1* (FLG22-INDUCED RECEPTOR-LIKE KINASE 1) and the flg22 receptor itself, *FLS2* (FLAGELLIN-SENSITIVE 2). RLKs are receptors that form the first line of defense in the plant immune system by transducing the perception of extracellular molecules into intracellular signals that activate immunity (24). Genes involved in the biosynthesis of secondary metabolites were also prevalent in cluster SC1. In particular, the master regulator of indole glucosinolate biosynthesis *MYB51* (25), along with three indole glucosinolate methyltransferases genes (*IGMT2*, *IGMT3*, and *IGMT4*) and various glutathione S-transferases and cytochrome P450s were not activated by flg22 in plants colonized by SynCom35 (*SI Appendix*, Fig. S2*H*). Root-exuded secondary metabolites act as chemical barriers against microbial invaders and suppression of their biosynthesis may favor colonization of microbial commensals (26). These results demonstrate that key components of the plant immune system, from receptors to transcription factors and biochemical executors, are modulated by SynCom35.

Since cluster SC1 overlaps significantly with a set of flg22-responsive genes that were suppressed by a different and independently derived SynCom from an independent study (*SI Appendix*, Fig. S3*A* and Dataset S3) (27), modulation of this sector of the plant immune system is likely to be a common strategy employed by root commensals. Cluster SC1 also overlaps significantly (84 of 281 genes; P = 3.27E-58) (Dataset S3) with a set of 868 genes that are flg22-regulated across four *Brassicaceae* species (28), indicating that SynCom35 has the potential to modulate an evolutionarily conserved sector of MTI. Although defense-related genes were not activated by flg22 in plants grown with SynCom35 at day 12, they were up-regulated on the first day of treatment (*SI Appendix*, Fig. S3 *B–F* and Dataset S3), indicating that SynCom35, once fully established, suppresses an ongoing immune response instead of preventing its activation.

The subset of flg22-activated genes that were not suppressed by SynCom35 at day 12 (clusters SC2 and SC4) (Fig. 1*F*) were enriched in root morphogenesis and differentiation processes (Fig. 1*H*). These genes were constitutively activated by SynCom35 even in the absence of flg22 (Fig. 1*G*). Impaired primary root elongation is a phenotype of plants exposed to flg22 (29), a phenotype that is also triggered by SynCom35 (*SI Appendix*, Fig. S4*A*). *Arthrobacter* strains present in SynCom35 affect root

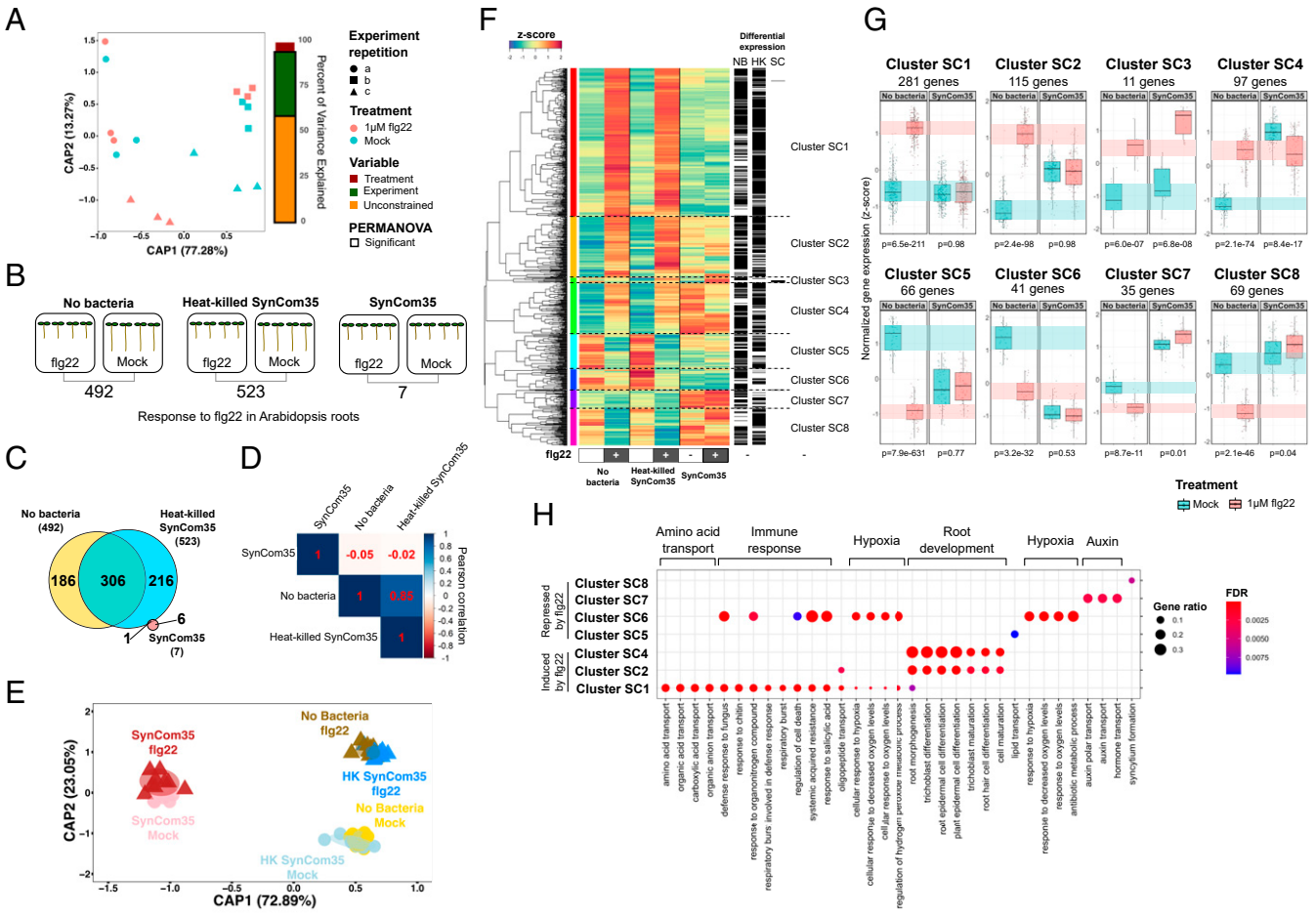

Fig. 1. A synthetic community comprised of 35 bacterial strains (SynCom35) modulates a sector of the *Arabidopsis* immune system. (*A*) Canonical analysis of principal coordinates (CAP) based on Bray–Curtis dissimilarities of 16S rDNA profiling reveals no significant effect of flg22 in the composition of root bacterial community. Significance of model terms was determined with a PERMANOVA analysis using 5,000 permutations ($\alpha = 0.05$). (*B*) Number of differentially expressed genes (DEG) identified by RNA sequencing in roots treated with flg22 or not in the absence of bacteria, with heat-killed SynCom35 or with SynCom35 alive. (*C*) Overlap among the sets of flg22-responsive genes in the "No bacteria," "Heat-killed SynCom35," and "SynCom35" conditions. (*D*) Pearson correlation among flg22 responses in plants grown axenically (no bacteria) or in the presence of dead or living SynCom35. Note the low correlation between "SynCom35" and the other two conditions. (*E*) CAP coordinates shows that plants grown in the presence of SynCom35 display a unique transcriptional signature that is not differentiated by addition of flg22. (*F*) Hierarchical clustering of the 716 genes that responded to flg22 in at least one of the experimental conditions. SynCom35 triggers a transcriptional signature that is very similar to the flg22 response except for three sets of genes (Cluster SC1, Cluster SC7, and Cluster SC8), which display a remarkably different expression profile when compared to control plants. (*G*) Expression pattern of each of the clusters defined in the heatmap. The *P* values on the bottom refer to the comparison between groups (flgs22 vs. mock) for each condition using two-tailed *t* tests. (*H*) Gene ontology enrichment analyses showing enriched biological processes in each of the clusters. Cluster SC1, which is suppressed by SynCom35, contains defense genes that are activated by flg22. Cluster SC7, which is activated by SynCom35, is enriched in auxin metabolism. All results refer to plants exposed to the treatments for 12 d. HK, heat-killed SynCom35; FDR, false-discovery rate; NB, no bacteria; SC, SynCom35. The complete enrichment analysis and the associated statistics are shown in Dataset S3.

development, likely via auxin production (30). Consistent with this observation, auxin-responsive genes were highly activated in plants grown with SynCom35 (cluster SC7 in Fig. 1 *F–H*). Furthermore, the auxin-resistant mutant *axr2-1* expressed a significantly reduced root growth-inhibition (RGI) phenotype in the presence of *Arthrobacter* MF161 (*SI Appendix*, Fig. S4*B*). These results demonstrate that the SynCom35 effect on root morphology is uncoupled from its immunomodulatory activity.

Dissecting the Immunomodulatory Activity of Commensals. After establishing that SynCom35 had immunomodulatory activity on *Arabidopsis* roots, we performed monoassociation experiments to evaluate the interaction of individual strains with the plant immune system. Seven-day-old *Arabidopsis* seedlings were inoculated with each member of SynCom35 in the presence or absence of 1 μM flg22 (*SI Appendix*, Fig. S5). Evaluation of root lengths revealed that individual strains interacted with the plants in three different ways (Fig. 2*A*). Twenty strains did not alter the flg22 effect on root morphology. Seven strains caused RGI even in the absence of flg22 (RGI inducers), a phenotype reminiscent of the SynCom35 effect on the plant. Importantly, eight strains suppressed the RGI phenotype triggered by flg22 (RGI suppressors), supporting longer root lengths in the presence of the MAMP. Because plants grown in the presence of SynCom35 display short roots (Fig. 2*A* and *SI Appendix*, Fig. S4*A*), the RGI inducers in this consortium are functionally dominant over the suppressors for this trait.

We next asked whether strains that suppressed flg22-mediated RGI were also efficient suppressors of the flg22 regulon. A principal component analysis (PCA) based on the expression of 428 genes that define the flg22 regulon in axenic plants

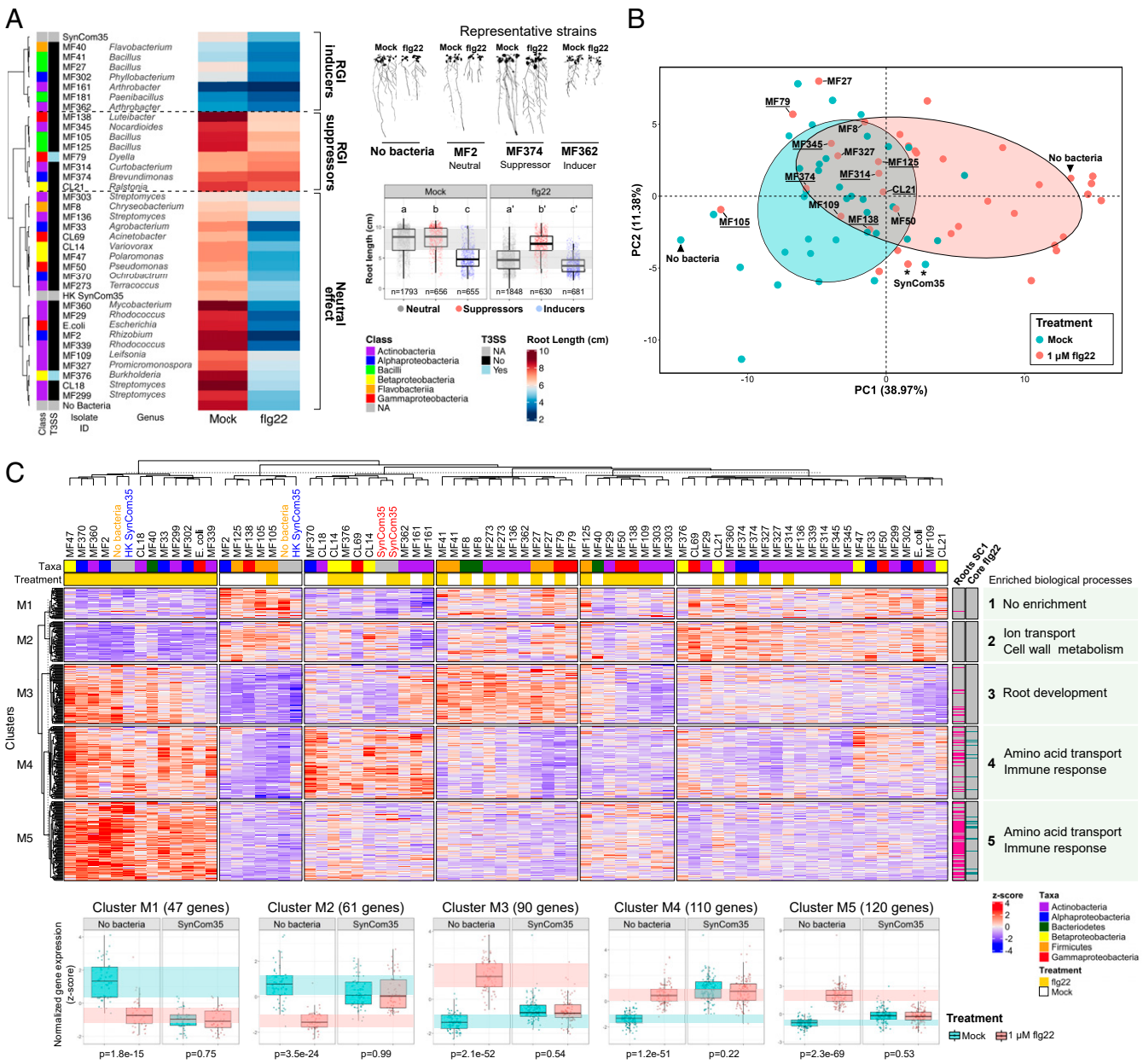

Fig. 2. Suppression of the flg22 response is a common feature among members of SynCom35. (*A*) *Arabidopsis* root length in the presence of each strain of SynCom35. While some strains have a neutral effect on the plant root elongation, others are able to suppress the flg22-induced RGI or induce the same phenotype even in the absence of flg22. The taxonomic class of each strain and the presence or not of a T3SS are annotated as colored boxes on the left of the heatmap. The images (*Right*) show the plant phenotype in the presence of a representative neutral (MF2), suppressor (MF374), and inducer strain (MF362). The boxplots summarize the effect of each group from the heatmap on root length (multiple comparisons were performed with ANOVA followed by a Tukey test, $\alpha = 0.05$). (*B*) PCA based on 428 genes that responded to flg22 in axenic plants demonstrates that some, but not all, strains of SynCom35 interfere with the transcriptional regulation of the flg22 regulon. Ellipses show the parametric smallest area around the mean that contains 70% of the probability mass for each group (blue: mock; red: 1 µM flg22). Only controls ("no bacteria" and "SynCom35") and suppressors of this gene set are labeled for clarity. Underlined labels indicate that the strain also suppressed the RGI phenotype triggered by flg22 shown in *A*. (*C*) Hierarchical clustering based on the expression of the same 428 genes in seedlings grown in the presence of each strain from SynCom35 along with controls (no bacteria, heat-killed SynCom35, and SynCom35). Five clusters were defined and their profiles in seedlings grown under axenic conditions or with SynCom35 are shown on the bottom. The *P* values refer to the comparison between groups (flg22 vs. mock) using two-tailed *t* tests. The boxes on the top of the heatmap indicate the taxonomic classification of the inoculated strain and treatment (orange) or not (white) with flg22. Lanes on the right of the heatmap indicate whether each gene was suppressed by SynCom35 in roots (cluster SC1) (Fig. 1*F*) or whether they belong to the set of 84 core flg22 marker genes (*SI Appendix*, Fig. S6). Representative biological processes that are enriched in each cluster are shown on the right. The complete enrichment analysis and the associated statistics are shown in Dataset S4.

(Dataset S4) revealed suppression of this transcriptional response by various members of SynCom35 (Fig. 2*B*), including all strains that suppressed flg22-mediated RGI (Fig. 2*A*). Thus, efficient suppression of the flg22 regulon predicts suppression of the flg22 effect on root elongation. This conclusion was validated using an orthogonal approach. We generated a literature-based core set of 84 flg22 transcriptional markers, defined by both chronic and acute flg22 treatments of diverse *Arabidopsis* tissues

(*SI Appendix*, Fig. S6 *A* and *B* and Dataset S5). These 84 genes contained 40 cluster SC1 genes (P = 2.82E-57) and 52 of the evolutionarily conserved flg22 regulon (28) (P = 9.34e-56). We clustered our data based on their expression (*SI Appendix*, Fig. S6*C*). The two resulting groups reflected the expression levels of these defense-related genes: Group I (*SI Appendix*, Fig. S6*C*, blue) displayed low expression of these marker genes and was mostly comprised of mock-treated plants; and group II (*SI Appendix*, Fig. S6*C*, red) presented higher expression of the same genes and was mostly comprised of flg22-treated plants. However, some strains prevented the activation of the flg22 core set when plants were exposed to the elicitor, while others activated the same genes even in the absence of flg22. These results show that the SynCom35 commensal consortium contains members that have opposing effects on the plant immune response to flg22.

To explore strain-specific effects on the plant immune response in more detail, the 428 flg22-responsive genes that were defined in axenic plants were subjected to hierarchical clustering based on their expression levels in the context of monoassociations (Fig. 2*C*). Eleven of the 35 strains (31%) had no effect on the plant response to flg22; seedlings grown in the presence of these bacteria responded to the MAMP similarly to seedlings grown without bacteria or with the heat-killed SynCom35 (Fig. 2*C*). The remaining 24 strains (69%) suppressed the plant transcriptional response to flg22 either partially or completely. Of the three clusters containing genes activated by flg22 (clusters M3, M4, and M5) (Fig. 2*C*), one was enriched in root development (cluster M3) (Fig. 2*C* and Dataset S4) and two were enriched in defense-related genes (clusters M4 and M5) (Fig. 2*C* and Dataset S4). Importantly, cluster M5 was the only set of flg22-responsive genes whose activation by the MAMP was consistently suppressed by all 24 strains, indicating that modulation of these defense-related genes is a common feature shared among phylogenetically diverse commensal bacteria. Cluster M5 is also highly overlapping (76 of 120 genes) with the cluster SC1 genes suppressed by SynCom35 in *Arabidopsis* roots (Figs. 1*F* and 2*C*, column labeled "Roots SC1").

Evaluation of the *Arabidopsis* transcriptome in response to each member of SynCom35 in the absence of exogenous MAMPs complemented the analyses focused on the flg22 response (*SI Appendix*, Fig. S7 *A* and *B*). Most strains (22 of 35) triggered the activation of defense-related genes to some extent (*SI Appendix*, Fig. S7*C*). However, activation of defense-related genes was undetectable in plants grown in the presence of the other, taxonomically diverse, 13 strains (*SI Appendix*, Fig. S7*C*). Eleven of these strains also suppressed cluster M5 of flg22-responsive genes in plants treated with flg22 (Fig. 2*C*). Thus, these results extend our observations and demonstrate that phylogenetically diverse commensals can modulate immune responses triggered by endogenous MAMPs.

We assessed the modulation of MTI by root commensals using an independent and conceptually distinct experimental system. Because flg22 triggers transcriptional responses in plant cells within minutes and over hours of its perception (15, 20, 21), we evaluated whether members of SynCom35 also interfere with the acute response that is triggered only 5 h after root exposure to flg22 using the same set-up that was previously employed to characterize MTI in the roots (19). For this, we utilized an *Arabidopsis* line carrying the *GUS* reporter gene under control of the flg22-responsive promoter *pCYP71A12*, which is activated by flg22 specifically in the root elongation zone (19). Plants treated with 100 nM flg22 under axenic conditions activated the *pCYP71A12* promoter in roots within 5 h of treatment. This response was absent in the control treatments [i.e., plants treated with 10 μM MeJA or with the *Pseudomonas simiae* strain WCS417 (19)] but was observed in plants inoculated with most of the members of SynCom35 (*SI Appendix*, Fig. S6*D*). Importantly, seven strains suppressed *pCYP71A12* activation by flg22 in this assay, indicating that these commensals can also interfere with the plant acute response to this MAMP.

By collating the results from the independent and conceptually different monoassociation experiments, a set of 10 robust MTI suppressors emerged within the members of SynCom35 (Fig. 3*A*). Although some strains of this community remained neutral or even activated the plant immune system in some assays, a total of 23 strains (65%) suppressed the plant response to flg22 in at least one assay (Fig. 3*A*). These results confirm that the ability to suppress the plant immune system is common and taxonomically widespread among root commensals. Interestingly, no strain among six tested robust suppressors modulated root immunity by lowering the extracellular pH (*SI Appendix*, Fig. S8*A*), a strategy recently described for commensal *Pseudomonas* (12). Interestingly, some suppressor strains interfered with the plant response to other peptide ligands and prevented RGI phenotypes induced by the damage-associated pep1 and developmental regulator clv3 peptides, while failing to suppress the RGI phenotype induced by hormones methyl jasmonate or auxin (*SI Appendix*, Fig. S8*B*). Thus, a diversity of extracellular MTI-suppression molecular mechanisms likely evolved among plant-associated bacteria in order to interfere with plant immunity.

MTI can Control Colonization by Commensals. We then tested the hypothesis that the ability to suppress the plant immune response is advantageous to commensal bacteria and, therefore, has ecological and evolutionary significance. We first evaluated the colonization ability of five robust suppressors and taxonomically matched strains from SynCom35 that did not suppress all measured outputs (Fig. 3*A* and Dataset S1). Monoassociation assays demonstrated that most suppressors grew to higher titers in *Arabidopsis* roots than nonsuppressors (Fig. 3*B*). This conclusion was supported by experiments using two smaller SynComs made of the five suppressors (SynCom5-S1) and five taxonomically matched nonsuppressors (SynCom5-NS1). In agreement with the monoassociation assays, 10-fold more bacterial colonies were recovered from *Arabidopsis* roots inoculated with SynCom5-S1 than with SynCom5-NS1 (Fig. 3*C*). The same result was obtained in an independent experiment that used different SynComs (SynCom5-S2 and SynCom5-NS2) (*SI Appendix*, Fig. S9 and Dataset S1). As predicted, seedlings inoculated with SynCom5-NS1 showed stronger activation of defense-related genes in comparison to seedlings inoculated with SynCom5-S1 (Fig. 3*D*, *SI Appendix*, Fig. S9 *B–E*, and Dataset S6). These genes encompass well-characterized components of the plant immune system, including those involved in the biosynthesis of glucosinolates, as well as RLKs and WRKYs (*SI Appendix*, Fig. S9*D*). Many of these genes were also found in clusters SC1 (Fig. 1*F*) and M5 (Fig. 2*C*). Thus, efficient suppression of MTI by commensals correlates with enhanced root colonization. Supporting this conclusion, suppressors were detected at higher relative abundances more often than nonsuppressors in roots colonized with SynCom35 (Fig. 3*E*). Furthermore, strains that we defined as robust suppressors were also classified as robust endophytic compartment colonizers in a previous study using SynCom35 (22), while strains that we classified as nonsuppressors were not (Fig. 3*B*).

Since suppressor and nonsuppressor strains co-occur in the root microbiota, we evaluated whether modulation of MTI by suppressors enhances the colonization ability of other commensal strains (Fig. 4*A*). For this, *Arabidopsis* seedlings were initially grown for 14 d in the presence of synthetic communities

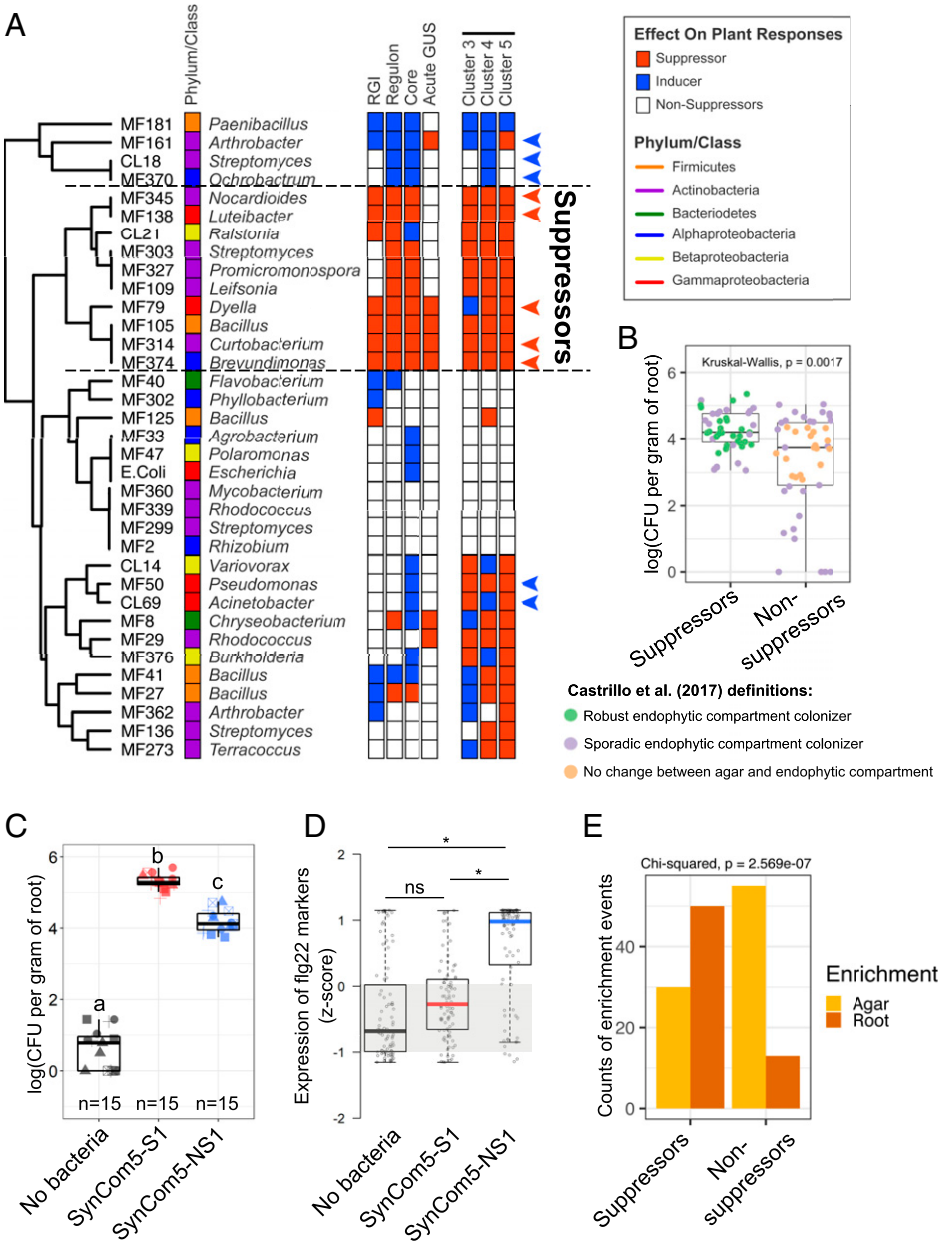

Fig. 3. Microbiota members that suppress the plant immune system are better colonizers of *Arabidopsis* roots either in monoassociation or in the context of SynComs. (*A*) Summary of the assays performed to define suppression of the flg22 response in this study. Strains are clustered based on their response to a total of five assays that are illustrated as rows of boxes to the right. RGI: the ability of a strain to suppress flg22-induced RGI or induce this phenotype even in the absence of the MAMP (Fig. 2*A*). Regulon: the ability to interfere with the overall expression signature of 428 flg22-responsive genes defined in control (no bacteria) seedlings (Fig. 2*B*). Core: the ability of each strain to interfere specifically with a set of 84 defense-related genes that are consistently induced by flg22 under diverse experimental conditions (*SI Appendix*, Fig. S6*C*). Acute GUS: the ability of each strain to interfere with the acute response to flg22 (5 h treatment) specifically in roots based on the *pCYP71A12::GUS* reporter line (*SI Appendix*, Fig. S6*D*). Clusters 3, 4, and 5: the suppression ability of each strain on specific transcriptional response sectors of the flg22 regulon (Fig. 2*C*). Members of SynCom5-S1 and SynCom5-NS1 are marked with red and blue arrowheads, respectively. (*B*) Suppressors are better colonizers of *Arabidopsis* roots in monoassociation experiments. The growth of five suppressors (members of SynCom5-S1) and taxonomically matching nonsuppressors (members of SynCom5-NS1) were individually assayed in *Arabidopsis* roots after 12 d of colonization in three biological replicates. Each dot represents an individual strain/replicate. Strains are colored based on their behavior in the context of SynCom35 in a previous study (22). Note that all robust endophytic compartment colonizers are suppressor strains. A Kruskal–Wallis test was performed on the CFU counts from three independent experiments each with three technical reps. $n = 9$ for each strain and $n = 45$ for each group being compared. (*C*) A SynCom made of five suppressors (SynCom5-S1) colonizes *Arabidopsis* roots better than a SynCom made of five taxonomically matching nonsuppressors (SynCom5-NS1). Different symbols represent independent experimental repetitions. Letters indicate significantly different groups based on an ANOVA followed by a Tukey test ($\alpha = 0.05$). (*D*) Seedlings grown with SynCom5-NS1 activate the expression of flg22 marker genes while seedlings inoculated with SynCom5-S1 do not. Statistical significance was determined using a permutation approach, where the actual group mean differences were compared to the group mean differences of 10,000 permutations of the gene counts. The group mean differences that were greater than 95% of the group mean differences calculated in the permutations were considered significant (asterisks). n.s. = not significant. (*E*) Suppressor (SynCom5-S1), but not nonsuppressor (SynCom5-NS1), strains are enriched in the endophytic compartment of *Arabidopsis* roots relative to agar in the context of a synthetic community. Suppressors $n = 80$, nonsuppressors $n = 68$.

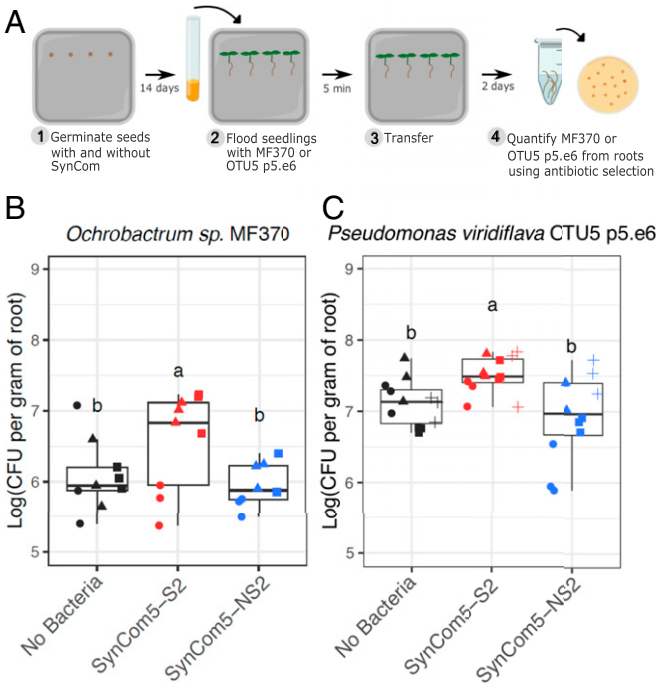

Fig. 4. Immunomodulatory bacteria enhance the root colonization ability of other commensal strains. (*A*) Cartoon representation of the experimental system employed. *Arabidopsis* seedlings were grown axenically, in the presence of a community of five suppressors (SynCom5-S2) or in the presence of five nonsuppressors (SynCom5-NS2) and then inoculated with one of the commensal strains. (*B*) Quantification of *Ochrobactrum* sp. MF370 cells (kanamycin resistant) from *Arabidopsis* roots ($n = 9$). (*C*) Quantification of *P. viridiflava* OTU5 p5.e6 cells (gentamycin resistant) from *Arabidopsis* roots ($n = 12$). Different symbols represent independent experimental repetitions. Multiple comparisons were performed with ANOVA followed by a Tukey test ($\alpha = 0.05$).

comprised of five suppressors (SynCom5-S2) or five nonsuppressors (SynCom5-NS2) (Dataset S1). Subsequently, plants were flood-inoculated for 5 min with the inducer *Ochrobactrum* sp. MF370 and grown for 48 h. More *Ochrobactrum* sp. MF370 cells were recovered from roots colonized with SynCom5-S2 compared to those inoculated with SynCom5-NS2 or grown axenically (Fig. 4*B*). The same result was observed for a second commensal microbe, *Pseudomonas viridiflava* OTU5 strain p5.e6 (Fig. 4*C*), which can also be an opportunistic plant pathogen (31). Thus, suppressor strains can enhance the root colonization capacities of other microbes, indicating that MTI, and its suppression, can contribute to the control of microbial loads in the roots.

Immunomodulatory Strategies in Commensals. Finally, we sought to identify the mechanism of suppression by one of the robust suppressor strains, *D. japonica* MF79 (Fig. 3*A*). This strain carries a T3SS, a molecular syringe that is widely employed by bacterial pathogens to inject virulence effectors into the cells of their hosts to suppress MTI (32). Thus, we tested the hypothesis that this commensal relies on the T3SS to interfere with plant immunity. We constructed two T3SS deletion strains and evaluated their ability to modulate the root response to flg22 using the *pCYP71A12::GUS* reporter line. The first mutant (MF79 *Δ*T3SS_RSTU) deletes the T3SS inner membrane components (*SctRSTU*), whereas the second mutant (MF79 *Δ*T3SS_full) deletes the full T3SS locus (*SI Appendix*, Fig. S10*A*). Interestingly, neither of these mutants were impaired in their ability to suppress the root response to flg22 (Fig. 5*A*). This demonstrates that the T3SS in this strain is dispensable for immune suppression.

To identify novel *D. japonica* MF79 genes required for the suppression activity, ∼4,500 strains from a transposon insertion library (33) were screened on the *pCYP71A12::GUS* reporter line in a high-throughput 96-well format. We found six mutant strains that were unable to suppress the activation of the *pCYP71A12::GUS* reporter by flg22 (Fig. 5*B*). Remarkably, all six transposon insertions mapped to the T2SS: one to the intracellular component *gspE* and five (four independent transposon hits, one duplicate) to the outer membrane component *gspD* (*SI Appendix*, Fig. S10*B* and Dataset S7). Thus, the T2SS is required for the secretion of substrates with immune suppressive activity to the extracellular space. Wild-type and mutant strains grew at the same rate in vitro (*SI Appendix*, Fig. S10*C*), suggesting that the loss of suppression ability in the *gspD* and *gspE* mutants is not merely due to growth defects. This was confirmed by experiments in which supernatants of bacteria grown in plant-free medium were used. Although no bacterial growth differences were observed in vitro, supernatant from wild-type *D. japonica* MF79 suppressed the root response to flg22, while neither the *gspD* nor *gspE* mutant supernatants had suppressive activity (Fig. 5*C*). The suppressive activity from wild-type *D. japonica* MF79 was retained by the filter of a 10-kDa protein concentrator, but not in the flow-through (Fig. 5*D*). Importantly, the 10-kDa retentate from wild-type *D. japonica* MF79 prevented the flg22-mediated reduction in root colonization of the nonsuppressor strain *Ochrobactrum* sp. MF370, and this effect required type 2 secretion components (Fig. 5*E*). Both the *gspD and* the *gspE* mutants were slightly poorer colonizers of *Arabidopsis* roots than the wild-type strain in monoassociation assays (*SI Appendix*, Fig. S10*D*). Taken together, these results suggest that suppression of the plant response to flg22 by *D. japonica* MF79 is mediated by at least one T2SS-secreted protein that is larger than 10 kDa and that the suppressive ability correlates with enhanced colonization of *Arabidopsis* roots.

Discussion

MTI is a well-known plant immune response to invading microbes, and its modulation by disease-causing pathogens has been extensively reported (10). Recent evidence suggests that the ability to suppress MTI has also evolved in commensal microbes (2). While previous studies focused on single microbes and on relatively simple MTI readouts, we demonstrate that a complex bacterial community of *Arabidopsis* root commensals interferes with a specific sector of the plant transcriptional response to the MAMP flg22 (cluster SC1) (Fig. 1 *F* and *G*). The suppression of these genes thus defines the set of host immune response genes that are likely modulated to facilitate successful commensal colonization. Suppression of subsets of MAMP-responsive genes has been observed in *Arabidopsis* roots colonized by the single commensal strains *P. simiae* WCS417 and *Bacillus subtilis* FB17 (15, 34). Although these studies did not investigate the effect of the microbes on the immune response elicited with exogenous MAMPs, they support our conclusion that diverse commensal bacteria interfere with specific sectors of the plant immune system. Thus, similar to what has been established for pathogenic microbes, suppression of the plant immune system is a hallmark of root colonization by commensals. Importantly, our findings agree with and significantly extend the proposal that the ability to suppress the host immune system is common and taxonomically widespread among root-associated bacteria (12, 13), a concept that has also emerged for human gut commensals (11). Recent evidence suggests that root commensals may avoid host cell damage, a signal that enhances MTI in

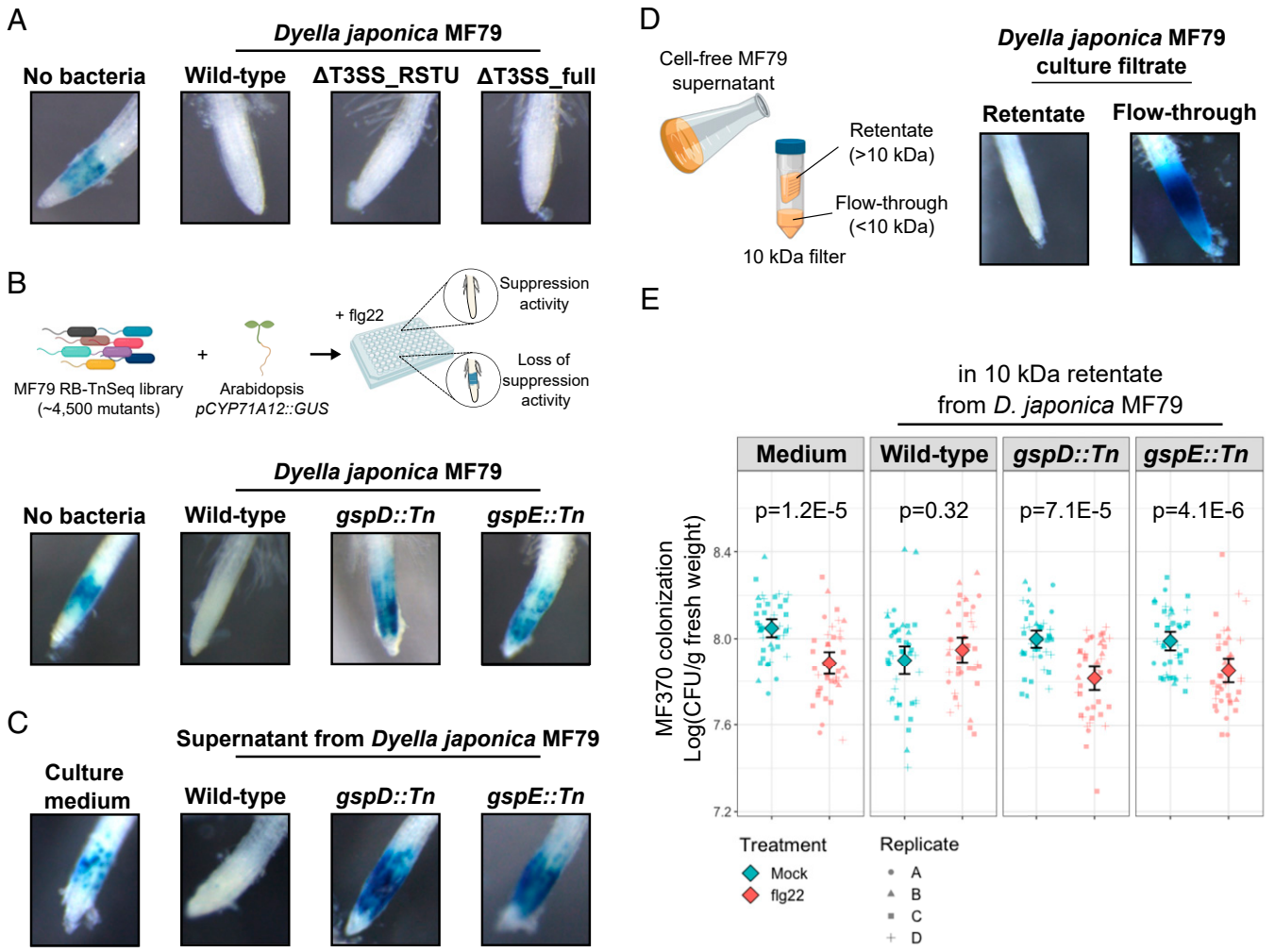

Fig. 5. *D. japonica* MF79 requires the T2SS to suppress the root response to flg22. (*A*) The T3SS is not required for MTI suppression by *D. japonica* MF79. Two independent mutants (ΔT3SS_RSTU and ΔT3SS_full) retained the ability to prevent activation of the *pCYP71A12::GUS* reporter in roots exposed to 100 nM flg22 for 5 h. (*B*) The screening of a transposon insertion library revealed two major components of the bacterial T2SS (GspD and GspE) as required for suppression of the root response to flg22. The diagram (*Upper*) summarizes the strategy employed in the screening. Additional mutants and replicates are shown in *SI Appendix*, Fig. S10*B*. (*C*) The cell-free supernatant of wild-type *D. japonica* MF79, but not of T2SS mutants, is sufficient for the suppression of the root response to flg22. (*D*) The molecule responsible for the suppression activity is larger than 10 kDa. The diagram (*Left*) illustrates the preparation of 10-kDa retentate and flow-through from bacterial cultures. (*E*) The 10-kDa retentate of wild-type *D. japonica* MF79 prevents the flg22-mediated reduction of *Ochrobactrum* sp. MF370 colonization. Four independent experiments were performed ($n = 42$ per condition). Diamonds represent means with two times SE. *P* values were determined with the Wilcoxon test. Root images were captured at 43× magnification on a Leica M205 FA fluorescence stereo microscope.

root tissues, to prevent the activation of plant immunity during colonization (8). Since we observed a clear response to flg22 in our control conditions (no bacteria and heat-killed SynCom35), suppression of defense-related genes in roots colonized by SynCom35 is not merely due to damage avoidance. It is noteworthy that the suppression of immune responses is a dominant trait in our SynCom.

A distinctive feature of our study is the dissection of the immunomodulatory capacity of 35 individual commensal strains and the integration of this information with the outcome observed in a community context. Monoassociation experiments revealed that root commensals trigger both shared and unique responses in *Arabidopsis*, without any obvious taxonomic signature (Fig. 2 and *SI Appendix*, Fig. S6). Interestingly, a common set of defense-related genes was suppressed by most strains (cluster M5) (Fig. 2*C*), indicating that phylogenetically diverse bacteria likely employ multiple mechanisms to exert a redundant immunomodulatory effect on the host. Many of these genes were also suppressed by a different bacterial community characterized in an independent study (*SI Appendix*, Fig. S3*A*) (27), supporting the hypothesis that root commensals manipulate a core set of biological processes in their hosts. Members of the WRKY family of transcription factors (e.g., *WRKY28*, *-30*, and *-33*) were consistently activated by flg22 in the roots, but suppressed by our strains and by those reported by Ma et al. (27) (*SI Appendix*, Fig. S3*A*). These *WRKYs* might constitute key regulators of the plant immune response to commensals, possibly playing important roles in the homeostasis of immune responses during commensal community assembly. Importantly, a robust, widespread, and redundant immunomodulatory capacity among commensals could buffer plant-associated communities against perturbations and maintain homeostasis when some members are lost or when external stimuli are present, as demonstrated for SynCom35 (Fig. 1*A*). Furthermore, the unique effect of each strain on the host may account for specific features, such as the ability to

prime the plant immune system or to trigger induced systemic resistance (35).

One hypothesis supported by our findings is that the presence of suppressor strains might benefit other nonsuppressors in the context of plant-associated communities. Although suppressors were often more efficient root colonizers than nonsuppressor strains, the latter (including *D. japonica* MF79 T2SS mutants) could still be recovered from *Arabidopsis* roots, either in mono-association or SynCom experiments. This indicates that suppression of the plant immune system likely facilitates bacterial growth within plant tissues but is unlikely to be a requirement for the colonization by most commensal strains. Interestingly, root colonization of nonsuppressive bacteria was enhanced by the presence of a suppressor SynCom (Fig. 4). We predict that this effect might involve specific, rather than general, microbial combinations. Niche occupancy and specific microbe–microbe interactions are important factors contributing to microbial colonization of plant tissues, resulting in different community contexts and complex phenotypes. It is interesting to note, however, that cell-free supernatant from wild-type *D. japonica* MF79, but not from T2SS mutants, prevented the flg22-mediated reduction in root colonization of the nonsuppressor strain *Ochrobactrum* sp. MF370 (Fig. 5*E*). This indicates that nonsuppressor bacteria can indeed benefit from the immunomodulatory activity of other community members under specific circumstances.

Our data suggest that the ability to suppress the plant immune system has evolved several independent times in plant commensals, likely resulting in numerous immunosuppressive mechanisms (2, 4). In contrast to most pathogens or mutualist microbes, root-associated commensals seem to display a much lower degree of host specialization. As a consequence, commensals may interfere with MTI mostly through nonspecific extracellular strategies. In turn, pathogens and specialized symbionts, such as nodule-forming rhizobia, often rely on highly specialized effector proteins that are injected into the host cell through the T3SS (36). Interestingly, *D. japonica* MF79 is the only suppressor commensal in SynCom35 to carry genes for the T3SS. Nevertheless, *D. japonica* MF79 *ΔT3SS* mutants retained their ability to suppress the flg22 response in *Arabidopsis* roots. Our transposon library screening resulted in six mutants in the T2SS, but no hits in other genes encoding putative T2SS substrates. This suggests that multiple proteins are secreted by *D. japonica* MF79 to the extracellular space and act redundantly to suppress MTI, consistent with previous demonstrations that T2SS can be required for pathogen virulence (37). Interestingly, only 3 of the 10 robust suppressors of the flg22 response (Fig. 3*A*) are predicted to carry a T2SS (Dataset S1), indicating the T2SS is dispensable for the suppression activity of most of these strains. We expect that new research will reveal a large number of novel strategies employed by commensals to modulate the plant immune system. Future studies should also elucidate the role of plant genes, specifically those in cluster SC1 (Fig. 1 *F* and *G*), in gating the assembly of microbial communities.

Materials and Methods

Details of the methods used in this work, including the preparation of bacterial synthetic communities, flg22 treatments, root length measurements, RNA extraction, RNA-sequencing analysis, DNA extraction, 16S amplicon sequencing, quantification of bacteria colonization of roots, GUS histochemical assays, genetic manipulation of bacteria, and mutant screenings, are described in *SI Appendix, SI Text, Materials and Methods*.

Data Availability. The data reported in this paper have been deposited in the Gene Expression Omnibus (GEO) database, https://www.ncbi.nlm.nih.gov/geo (accession no. GSE156426).

ACKNOWLEDGMENTS. We thank Dr. Ka-Wai Ma and Dr. Paul Schulze-Lefert for providing the gentamycin-resistant *Pseudomonas viridiflava* strain OTU5 p5.e6 and for sharing their bacteria colonization protocol and unpublished transcriptome data; Schulze-Lefert laboratory members for comments on the manuscript; the J.L.D. laboratory microbiome group for useful discussions; and Prof. Sarah Grant for comments and suggestions on the manuscript. This work was supported by NSF Grant IOS-1917270 and by Office of Science (Biological and Environmental Research), US Department of Energy Grant DE-SC0014395 (to J.L.D.) J.L.D is an Investigator of the Howard Hughes Medical Institute (HHMI), supported by the HHMI. P.J.P.L.T. was supported by The Pew Latin American Fellows Program in the Biomedical Sciences. N.R.C. was supported by NIH Training Grant T32GM135123.

1. C. R. Fitzpatrick *et al*., The plant microbiome: From ecology to reductionism and beyond. *Annu. Rev. Microbiol.* **74**, 81–100 (2020).
2. P. J. P. Teixeira, N. R. Colaianni, C. R. Fitzpatrick, J. L. Dangl, Beyond pathogens: Microbiota interactions with the plant immune system. *Curr. Opin. Microbiol.* **49**, 7–17 (2019).
3. K. Yu, C. M. J. Pieterse, P. A. H. M. Bakker, R. L. Berendsen, Beneficial microbes going underground of root immunity. *Plant Cell Environ.* **42**, 2860–2870 (2019).
4. S. Hacquard, S. Spaepen, R. Garrido-Oter, P. Schulze-Lefert, Interplay between innate immunity and the plant microbiota. *Annu. Rev. Phytopathol.* **55**, 565–589 (2017).
5. S. L. Lebeis *et al*., PLANT MICROBIOME. Salicylic acid modulates colonization of the root microbiome by specific bacterial taxa. *Science* **349**, 860–864 (2015).
6. J. M. Kniskern, M. B. Traw, J. Bergelson, Salicylic acid and jasmonic acid signaling defense pathways reduce natural bacterial diversity on *Arabidopsis thaliana*. *Mol. Plant Microbe Interact.* **20**, 1512–1522 (2007).
7. T. Chen *et al*., A plant genetic network for preventing dysbiosis in the phyllosphere. *Nature* **580**, 653–657 (2020).
8. F. Zhou *et al*., Co-incidence of damage and microbial patterns controls localized immune responses in roots. *Cell* **180**, 440–453.e18 (2020).
9. A. Emonet *et al*., Spatially Restricted Immune Responses Are Required for Maintaining Root Meristematic Activity upon Detection of Bacteria. *Curr Biol* **31**, 1012–1028.e7, 10.1016/j.cub.2020.12.048 (2021).
10. L. da Cunha, M.-V. Sreerekha, D. Mackey, Defense suppression by virulence effectors of bacterial phytopathogens. *Curr. Opin. Plant Biol.* **10**, 349–357 (2007).
11. N. Geva-Zatorsky *et al*., Mining the human gut microbiota for immunomodulatory organisms. *Cell* **168**, 928–943.e11 (2017).
12. K. Yu *et al*., Rhizosphere-associated *Pseudomonas* suppress local root immune responses by gluconic acid-mediated lowering of environmental pH. *Curr. Biol.* **29**, 3913–3920.e4 (2019).
13. R. Garrido-Oter *et al*.; AgBiome Team, Modular traits of the Rhizobiales root microbiota and their evolutionary relationship with symbiotic Rhizobia. *Cell Host Microbe* **24**, 155–167.e5 (2018).
14. Z. Liu *et al*., A genome-wide screen identifies genes in rhizosphere-associated *Pseudomonas* required to evade plant defenses. *MBio* **9**, e00433-18 (2018).
15. I. A. Stringlis *et al*., Root transcriptional dynamics induced by beneficial rhizobacteria and microbial immune elicitors reveal signatures of adaptation to mutualists. *Plant J.* **93**, 166–180 (2018).
16. J. M. Plett *et al*., Effector MiSSP7 of the mutualistic fungus *Laccaria bicolor* stabilizes the Populus JAZ6 protein and represses jasmonic acid (JA) responsive genes. *Proc. Natl. Acad. Sci. U.S.A.* **111**, 8299–8304 (2014).
17. Y. Liang *et al*., Nonlegumes respond to rhizobial Nod factors by suppressing the innate immune response. *Science* **341**, 1384–1387 (2013).
18. V. Lakshmanan *et al*., Microbe-associated molecular patterns-triggered root responses mediate beneficial rhizobacterial recruitment in Arabidopsis. *Plant Physiol.* **160**, 1642–1661 (2012).
19. Y. A. Millet *et al*., Innate immune responses activated in Arabidopsis roots by microbe-associated molecular patterns. *Plant Cell* **22**, 973–990 (2010).
20. G. Rallapalli *et al*., EXPRSS: An Illumina based high-throughput expression-profiling method to reveal transcriptional dynamics. *BMC Genomics* **15**, 341 (2014).
21. C. Denoux *et al*., Activation of defense response pathways by OGs and Flg22 elicitors in Arabidopsis seedlings. *Mol. Plant* **1**, 423–445 (2008).
22. G. Castrillo *et al*., Root microbiota drive direct integration of phosphate stress and immunity. *Nature* **543**, 513–518 (2017).
23. P. J. Rushton, I. E. Somssich, P. Ringler, Q. J. Shen, WRKY transcription factors. *Trends Plant Sci.* **15**, 247–258 (2010).
24. D. Couto, C. Zipfel, Regulation of pattern recognition receptor signalling in plants. *Nat. Rev. Immunol.* **16**, 537–552 (2016).
25. T. Gigolashvili *et al*., The transcription factor HIG1/MYB51 regulates indolic glucosinolate biosynthesis in *Arabidopsis thaliana*. *Plant J.* **50**, 886–901 (2007).
26. A. Pascale, S. Proietti, I. S. Pantelides, I. A. Stringlis, Modulation of the root microbiome by plant molecules: The basis for targeted disease suppression and plant growth promotion. *Front. Plant Sci.* **10**, 1741 (2020).

27. K.-W. Ma *et al*., Coordination of microbe-host homeostasis by crosstalk with plant innate immunity. *Nature Plants*, 10.1038/s41477-021-00920-2 (2021) in press.
28. T. M. Winkelmüller *et al*., Gene expression evolution in pattern-triggered immunity within *Arabidopsis thaliana* and across Brassicaceae species. *bioRxiv* (2020).
29. L. Gómez-Gómez, G. Felix, T. Boller, A single locus determines sensitivity to bacterial flagellin in Arabidopsis thaliana. *Plant J.* **18**, 277–284 (1999).
30. O. M. Finkel *et al*., A single bacterial genus maintains root growth in a complex microbiome. *Nature* **587**, 103–108 (2020).
31. T. L. Karasov *et al*., *Arabidopsis thaliana* and *Pseudomonas* pathogens exhibit stable associations over evolutionary timescales. *Cell Host Microbe* **24**, 168–179.e4 (2018).
32. W. Deng *et al*., Assembly, structure, function and regulation of type III secretion systems. *Nat. Rev. Microbiol.* **15**, 323–337 (2017).
33. M. N. Price *et al*., Mutant phenotypes for thousands of bacterial genes of unknown function. *Nature* **557**, 503–509 (2018).
34. V. Lakshmanan, R. Castaneda, T. Rudrappa, H. P. Bais, Root transcriptome analysis of *Arabidopsis thaliana* exposed to beneficial *Bacillus subtilis* FB17 rhizobacteria revealed genes for bacterial recruitment and plant defense independent of malate efflux. *Planta* **238**, 657–668 (2013).
35. C. Vogel, N. Bodenhausen, W. Gruissem, J. A. Vorholt, The Arabidopsis leaf transcriptome reveals distinct but also overlapping responses to colonization by phyllosphere commensals and pathogen infection with impact on plant health. *New Phytol.* **212**, 192–207 (2016).
36. B. Gourion, F. Berrabah, P. Ratet, G. Stacey, Rhizobium-legume symbioses: The crucial role of plant immunity. *Trends Plant Sci.* **20**, 186–194 (2015).
37. N. P. Cianciotto, R. C. White, Expanding role of type II secretion in bacterial pathogenesis and beyond. *Infect. Immun.* **85**, e00014-17 (2017).

PNAS
www.pnas.org

Supplementary Information for

Specific modulation of the root immune system by a community of commensal bacteria

Paulo J. P. L. Teixeira, Nicholas R. Colaianni, Theresa F. Law, Jonathan M. Conway, Sarah Gilbert, Haofan Li, Isai Salas-González, Darshana Panda, Nicole M. Del Risco, Omri M. Finkel, Gabriel Castrillo, Piotr Mieczkowski, Corbin D. Jones, Jeffery L. Dangl*

* To whom correspondence should be addressed.
Email: dangl@email.unc.edu

This PDF file includes:

Supplementary text
Figures S1 to S10
SI References

Other supplementary materials for this manuscript include the following:

Datasets S1 to S7

Supplementary Information Text

Materials and Methods

Preparation of bacterial synthetic communities (SynComs). We employed SynComs to evaluate the effect of the root microbiota on plant immune responses. A 35-member SynCom (SynCom35) was assembled using a set of genome-sequenced strains that represent the typical taxonomic diversity of plant-associated bacteria (1). This SynCom included 32 strains that were isolated from *Brassicaceae* roots (mainly Arabidopsis), two strains that were isolated from unplanted soil (Mason Farm - North Carolina, USA; +35° 53′ 30.40″, −79° 1′ 5.37″) and *Escherichia coli* DH5α as a control. Smaller SynComs were assembled with subsets of strains from this 35-member SynCom (i.e., SynCom5-S: five suppressors; and SynCom5-NS: five non-suppressors). A detailed description of the strains that comprise the SynComs used in this study is provided in SI Appendix, Dataset 1.

Assembly of SynComs followed the procedures described by Castrillo et al. (1). Briefly, a single colony of each strain was inoculated into 4 mL 2xYT medium (16 g/L tryptone, 10 g/L yeast extract and 5 g/L NaCl) in a test tube and kept at 28°C under agitation at 250 rpm. After one to two days, bacterial cultures were washed twice with 10 mM $MgCl_2$ (by centrifugation and resuspension) and OD_{600nm} was determined by spectrophotometry. Cultured bacterial strains were then added to 500 mL of medium to a final concentration of 10^5 cfu/mL each (assuming that one OD_{600nm} unit equals to 10^9 cfu/mL). In some experimental conditions, the bacterial elicitor flagellin 22 (flg22) was added along with bacteria at a final concentration of 1 µM (described below).

Preparation of plants for bacteria and flg22 treatments. *Arabidopsis thaliana* seeds (ecotype Columbia; Col-0) were surface-sterilized with a cleaning solution (70% bleach and 0.2% Tween-20) for 8 min and rinsed three times with sterile distilled water to eliminate any seed-borne microbes on the seed surface. After stratification at 4°C for 2 days in the dark, seeds were transferred to square plates containing Johnson medium (5 g/L sucrose; 85 mg/L KH_2PO_4; 0.6 g/L KNO_3; 0.9 g/L $Ca(NO_3)_2{\cdot}4H_2O$; 0.2 g/L $MgSO_4{\cdot}7H_2O$; 3.8 mg/L KCl; 1.5 mg/L H_3BO_3; 0.8 mg/L $MnSO_4{\cdot}H_2O$; 0.6 mg/L $ZnSO_4{\cdot}7H_2O$; 0.1 mg/L $CuSO_4{\cdot}5H_2O$; 16.1 µg/L H_2MoO_4; 1.1 mg/L $FeSO_4{\cdot}7H_2O$; 0.1 g/L Myo-Inositol; 0.5 g/L MES; pH 5.6–5.7) solidified with 1% bacto-agar. Plates were kept in the vertical position for seven days in a growth chamber under a 16-hour light/8-hour dark regime at 21°C day/18°C night. The resulting seedlings were then ready for experiments.

Treatment of plants with flg22 in the presence of SynComs. We evaluated the effect of SynCom35 on the plant response to flg22 (Fig. 1) by cultivating plants in Johnson medium with or

without 1 µM of flg22 (synthesized by PhytoTech Labs) in the presence or not of the SynCom (inoculum: 10^5 cfu/mL of each strain; prepared as described above). A control condition in which plants were exposed to the heat-killed SynCom was included in the experiment by heating the bacteria at 100°C for 2h in an oven immediately before inoculating them into the medium at the same concentration as the SynCom alive. The complete design of this experiment as well as the parameters measured are shown in SI Appendix, Fig. S1.

Seven-day-old seedlings were obtained by germinating the seeds in Johnson medium as described above and then transferred to the six different experimental conditions (SI Appendix, Fig. S1). Plates were kept in a growth chamber under a 9-hour light/15-hour dark regime at 21°C day/18°C night. The entire root system of the seedlings was harvested for RNA extraction at two time-points: 1 and 12 days after the transfer to the treatment plates. Tubes were stored at −80°C until processing. The experiment included 9 biological replicates per condition, which were sub-divided into 3 batches (each containing 3 replicates per condition) that were performed independently (i.e., different days, medium, seedlings and bacterial inoculum). Each replicate corresponds to the root systems of ten seedlings grown in a single plate.

Treatment of plants with flg22 in the presence of individual strains. We evaluated the effect of each member of SynCom35 on the plant response to 1 µM flg22 in the context of mono-associations (Fig. 2 and SI Appendix, Fig. S5). For this, each strain was cultured and added individually to 500 mL of medium as described above at a concentration of 10^5 cfu/mL. Treatment of seedlings with flg22 in mono-association was performed as described for SynCom35 (see above). Seven-day-old seedlings were transferred to the different conditions of the experiment and harvested after 12 days for RNA extraction. Tubes were stored at −80°C until processing. The experiment included 9 biological replicates per condition, which were sub-divided into 3 batches (each containing 3 replicates per condition) that were performed independently (i.e., different days, medium, seedlings and bacterial inoculum). Each replicate corresponds to ten seedlings grown in a single plate. SI Appendix, Fig. S5 summarizes the design of this experiment.

Root length measurements. Before harvesting samples for RNA extraction at day 12 (end of the experiments), plates were scanned, and the root length of each seedling (10 per plate) was determined using ImageJ (2). Results from the SynCom35 experiment (Fig. 1 and SI Appendix, Fig. S4) were visualized with a boxplot made in R using the ggplot2 package (3). Due to the large number of treatments (i.e., strains) in the mono-association experiment (Fig. 2), results were visualized with a heatmap. For this, the raw root length data was fit with a linear model using the lm function in R. We identified a significant batch effect using the model:

$$Root\_length \sim Bacteria * flg22 + Batch$$

“Root_length” is the root length from each replicate, “Bacteria” is the strain inoculated into the plant growth medium, “flg22” is the presence of 1 µM flg22 or not, and “Batch” is the experimental effect (i.e., each of three independent batches of the experiment). To correct the root lengths for the batch effect, we used the beta effects of bacteria, flg22, and bacteria:flg22 from the linear model to calculate fitted root length measurements for each bacterial strain, one with flg22 and one without. These fitted measurements were then clustered using a Euclidean distance matrix and the ward.d2 clustering method implemented in the hclust function in R. The data was plotted with the R package ComplexHeatmap (4). The heatmap was annotated to indicate the Class of each strain as well as the presence or not of a type-3 secretion system (T3SS), which was predicted using macsyfinder and hidden Markov Models described by Abby et al. (5). The code used for this analysis can be found at GitHub (https://github.com/ncolaian/MAE).

RNA extraction and RNA-seq library preparation. Total RNA was extracted following the procedures described by Logemann et al. (6). Frozen plant tissue was pulverized inside a 2 mL tube containing three 4 mm glass beads using a Qiagen TissueLyser II instrument. Samples were homogenized in 400 µL of Z6-buffer (8 M guanidinium- HCl, 20 mM MES, 20 mM EDTA, pH 7.0). Following the addition of 400 µL phenol:chloroform:isoamyl alcohol (25:24:1), samples were vortexed and centrifuged (20,000 *g*, 10 min) for phase separation. The aqueous phase was transferred to a new 1.5 mL tube and 0.05 volumes of 1 N acetic acid and 0.7 volumes 96% ethanol were added. The RNA was precipitated at −20 °C overnight. Following centrifugation (20,000 *g*, 10 min, 4 °C) the pellet was washed with 200 µL sodium acetate (pH 5.2) and then 70% ethanol. The RNA was dried and dissolved in 30 µL of ultrapure water and stored at −80 °C until use.

Illumina mRNA-seq libraries were prepared from 1,000 ng RNA using the protocol described by Castrillo et al. (1). Briefly, mRNA was purified from total RNA using Sera-mag oligo(dT) magnetic beads (GE Healthcare Life Sciences) and then fragmented in the presence of divalent cations (Mg^{2+}) at 94°C for 6 min. The resulting fragmented mRNA was used for first-strand cDNA synthesis using random hexamers (ThermoFisher Scientific) and the EnzScript reverse transcriptase (Enzymatics), followed by second strand cDNA synthesis using DNA polymerase I (Enzymatics) and RNaseH (Enzymatics). Double-stranded cDNA was end-repaired using T4 DNA polymerase (Enzymatics), T4 poly-nucleotide kinase (Enzymatics) and Klenow polymerase (Enzymatics). The DNA fragments were then adenylated using Klenow exo-polymerase (Enzymatics) to allow the ligation of Illumina Truseq HT adapters (D501–D508 and D701–D712). Following library preparation, quality control and quantification were performed using a 2100 Bioanalyzer instrument (Agilent) and the Quant-iT PicoGreen dsDNA Reagent (ThermoFisher Scientific), respectively. Libraries were sequenced on the Illumina HiSeq4000 instrument to generate 50-bp single-end reads. A total of 100 and 666 libraries were produced for the SynCom35 (Fig. 1) and the mono-

association (Fig. 2) experiments, respectively. SI Appendix, Datasets 3 and 4 present details about each sample included in these experiments.

Processing of RNA-seq reads. Initial quality assessment of raw sequences was done with FastQC version 0.11.7 (Babraham Bioinformatics, Cambridge, UK). Trimmomatic version 0.36 (7) was used to remove adaptor-containing and low-quality sequences with parameters set at ILLUMINACLIP:TruSeq3-SE.fa:2:30:10, SLIDINGWINDOW:4:5, LEADING:5, TRAILING:5, MINLEN:50. The resulting high-quality reads were then aligned against the TAIR10 Arabidopsis reference genome using HiSat2 version 2.1.0 (8) using default parameters. The featureCounts function from the Sub-read package version 1.6.3 (9) was used to count reads that mapped to each one of the 27,206 nuclear protein-coding genes. Evaluation of the results of each step of the analysis was done with MultiQC version 1.7 (10). Raw RNA-seq reads and the count matrices generated in this study are available at the NCBI Gene Expression Omnibus under the accession number GSE156426.

Evaluation of the transcriptional response to flg22 in plants growing in the presence of SynComs. Identification of differentially expressed genes was performed using the generalized linear model (glm) approach (11) implemented in the R package edgeR (12). In the SynCom35 experiment (Fig. 1), weakly expressed genes were filtered out by removing those genes that did not achieve a minimum expression level of 1 count per million in at least five libraries. Normalization was performed using the trimmed mean of M-values method (TMM; function calcNormFactors in edgeR) (13). The glmFit function was used to fit the counts to a negative binomial generalized linear model with a log link function. In this experiment, our goal was to evaluate the root transcriptional response to flg22 in plants grown in the presence of the SynCom35 (alive or dead) or in the absence of bacteria (Fig. 1*B*). For this, we employed a one-way-layout model to compare each treatment ('no bacteria.flg22', 'SynCom35.flg22' or 'heat-killed SynCom35.flg22') to its control condition ('no bacteria.mock, 'SynCom35.mock' or 'heat-killed SynCom35.mock') at each time-point (T1h and T12h). The model included the covariate 'Experiment' to control for batch effects associated with the three independent repetitions of the experiment. The Benjamini–Hochberg method (false discovery rate; FDR) was used for the correction of multiple comparisons (14). Genes with an FDR corrected p-value below or equal to 0.01 and a fold-change of at least 1.5x were considered differentially expressed. We compared the sets of differentially expressed genes in each condition ('no bacteria', 'SynCom' and 'Heat-killed SynCom') using a Venn diagram (15) (Fig. 1*C*). Pearson correlations of flg22 responses (Fig. 1*D*) were estimated by comparing the fold-changes of all 715 genes that responded to flg22 in any of our conditions using the R package corrplot (16). A Constrained Analysis of Principal Coordinates (CAP) was performed to allow the visualization of the relative effects of our experimental conditions on the plant transcriptome (Fig. 1*E*). For this, we

selected the 500 genes with the highest standard deviation across all samples from the matrix of normalized gene counts generated by edgeR and used the capscale function from the vegan package (17) to compute the CAP. We constrained the ordination on the presence of the SynCom and the addition of flg22, while conditioning for the batch effect. Hierarchical clustering (Fig. 1*F* and SI Appendix, Fig. S3*C*) was performed with the 'heatmap.2′ function from the R package gplots (18) using those genes that responded to flg22 in at least one condition of the experiment (i.e, 'no bacteria', 'SynCom35' or 'Heat-killed SynCom35') within each time-point. Genes were clustered on the basis of the Euclidean distance with the complete-linkage method. The cutree function was used to define eight clusters based on dendrogram distances. To generate a representative view of each cluster (Fig. 1*G*), RPKM expression values were normalized by z-score transformation and presented in a boxplot. Gene Ontology (GO) enrichment analyses (Fig. 1*H* and SI Appendix, Figs S1 and S3) were performed with the compareCluster function of the R package clusterProfiler (19) and with the PlantGSEA platform (20).

Evaluation of the transcriptional response to flg22 in plants growing in the presence of individual strains. In the mono-associations experiment (Fig. 2), weakly expressed genes that did not have greater than 1 count per million in at least five libraries were removed from subsequent analyses. We then normalized the gene count matrix using the weighted trimmed mean of M-values (TMM) implemented in the calcNormFactors function from edgeR. We were interested in identifying (1) the plant genes that respond to bacteria in mono-association (bacteria_mock vs axenic_mock); and (2) plant genes that respond to flg22 in the presence of each strain in mono-association (bacteria_flg22 vs bacteria_mock) or in the 'no bacteria' control (axenic_flg22 vs axenic_mock). To perform these comparisons, we first subset the raw gene count table to only include the conditions being tested and created a DGEList object with this data using edgeR. We normalized the counts based on normalization factors calculated from the full gene count table. We then estimated the gene-wise dispersion parameters within each of the smaller datasets using the estimateGLMCommonDisp, estimateGLMTrendedDisp and estimateGLMTagwiseDisp functions from edgeR. Our design matrices were as follows for each of the contrasts listed above:

(1) expression ~ bact*experiment

(2) expression ~ treatment+experiment

"bact" is the bacterial strain, "experiment" is the batch effect (i.e., each of the three independent repetitions of the experiment), and "treatment" is the flg22 status. We then fit a gene-wise negative binomial generalized linear model with our calculated dispersion parameters using the glmFit function. After fitting the models, we conducted gene-wise log ratio tests contrasting our factor of

interest, (1) bacterial strain and (2) flg22 added, to the controls: (1) 'no bacteria' and (2) 'no flg22 added' using the glmLRT function. We used the decideTestsDGE function in edgeR to calculate FDR corrected p-values and report differentially expressed genes that had a log fold-change of at least 1.5 and an FDR corrected p-value of less than 0.01.

Principal Component Analysis (PCA) was performed with the set of 428 flg22-responsive genes defined in the control condition of the experiment (i.e., plants growing in the absence of bacteria) using the median expression values from the normalized counts matrix (log-transformed counts per million; with a prior count of 1) of the nine biological replicates from each condition. The function PCA from the R package AMOR (21) was employed with default parameters. The ellipses were defined using a multivariate t-distribution with a 70% confidence level. Code used for all analysis is found at https://github.com/ncolaian/mae.

DNA extraction for 16S sequencing. Plants were grown using MS medium (0.5X Murashige and Skoog basal medium with vitamins at pH 5.7 solidified with 1% bacto-agar) under the conditions and treatments described previously. Five roots were pooled and placed in 2.0 mL tubes with three sterile 4 mm glass beads. Samples were vortexed rigorously three times in sterile distilled water to remove agar particles and weakly associated microbes. Tubes containing the samples were stored at -80˚C until processing. Agar from each plate was collected in 30 mL syringes with a square of sterilized Miracloth (Millipore) at the bottom and stored at -20 °C until processing. Root samples were lyophilized for 48 hours using a Labconco freeze dry system and pulverized for 45 s in a FastPrep-24 Classic Instrument (MP Biomedicals). Agar containing syringes were thawed at room temperature and samples were squeezed gently through the Miracloth into 50 mL falcon tubes. Samples were centrifuged at max speed for 20 min and most of the supernatant was discarded. The remaining 1-2 mL of supernatant, containing the pellet, was transferred into clean 2 mL tubes. Samples were centrifuged again, supernatant was removed, and pellets were stored at -80 °C until DNA extraction. DNA extractions were carried out on ground root and agar pellets using 96-well format MoBio PowerSoil Kit (MOBIO Laboratories; Qiagen) following the manufacturer's instruction.

16S rDNA Sequencing Preparation. We amplified the V3-V4 regions of the bacterial 16S rRNA gene using the primers 357F (5′-TCGTCGGCAGCGTCAGATGTGTATAAGAGACAG**CCTACGGGAGGCAGCAG**-3′) and 806R (5′-GTCTCGTGGGCTCGGAGATGTGTATAAGAGACAG**GGACTACHVGGGTWTCTAAT**-3′).
Each PCR reaction was performed in triplicate. PCR conditions were as follows with the Kapa HiFi Hotstart readymix: 1.2 µL Kapa Buffer, 0.18 µL dNTPs, 0.3 µL DMSO, 0.12 µL Kapa HiFi Polymerase, 0.3 µL 10 µM 357F, 0.3 µL 10 µM 806R, 0.9 µL mixed plant rRNA gene-blocking

peptide nucleic acids (PNAs; 1:1 mix of 10 µM plastid PNA and 10 µM mitochondrial PNA), 1.7 µL dH_2O, 1 µL DNA; temperature cycling: 95°C for 5 min; 28 cycles of 98°C for 20 s; 78°C (PNA) for 15 s; 55°C for 15 s; 72°C for 1 min; 4°C until use. Triplicate PCR products were pooled and then diluted twice; 2 µL of PCR products into 18 µL of dH20 and 5 µL of Dilution 1 into 45 µL of dH_2O. Following dilution, the PCR product was indexed using 16 indexed primers 357F (5'-AATGATACGGCGACCACCGAGATCTACACXXXXXXXXTCGTCGGCAGCGTC-3') and 24 indexed primers 806R (5'-CAAGCAGAAGACGGCATACGAGATXXXXXXXXGTCTCGTGGGCTCGG-3'). PCR conditions were as follows with the Kapa HiFi Hotstart readymix: 2 µL Kapa Buffer, 0.3 µL dNTPs, 0.5 µL DMSO, 0.2 µL Kapa HiFi Polymerase, 0.5 µL 10 µM 357F index, 0.5 µL 10 µM 806R index, 0.15 µL PNAs; 1:1 mix of 100 µM plastid PNA and 100 µM mitochondrial PNA), 0.85 µL dH2O, 5 µL DNA; temperature cycling: 95°C for 5 min; 10 cycles of 98°C for 20 s; 78°C (PNA) for 15 s; 55°C for 15 s; 72°C for 1 min; 4°C until use. PCR products were purified using Sera-mag SpeedBeads (Fisher # 09-981-123) and quantified with a Qubit 2.0 fluorometer (Invitrogen) and then diluted to 6 pM for sequencing. Sequencing was performed on an Illumina MiSeq instrument using a 600- cycle V3 chemistry kit with 10% PhiX.

Analysis of the 16S sequencing data. Raw reads were trimmed with trimmomatic version 0.36 (7) using the parameters "HEADCROP:10 LEADING:3 TRAILING:3 SLIDINGWINDOW:4:15". Due to poor-quality base outputs in the beginnings and ends of reads we used headcrop and the leading/trailing trimming procedures. The sliding window command trims reads after the mean of 4 continuous base pairs reaches below a mean of 15. Once filtered, the resulting paired reads were analyzed using the DADA2 package version 1.14.1 (22) in R using the custom script code_for_16S_analysis.Rmd (https://github.com/ncolaian/MAE). Briefly, reads were filtered again by removing sequences containing uncalled bases, truncating reads after bases with a quality score of 2 and reads with no more than 3 expected errors using the FlilterAndTrim function in DADA2. We then learned the error rates for the forward and reverse reads separately with the learnErrors function. These error rates were then used to infer amplicon sequence variants (ASVs) with the function dada on the reverse and forward reads separately. After, we merged the forward and reverse strand results with the mergePairs function. The merged ASVs were used to construct an ASV sequencing table with only ASVs between 420 and 450 bp long, which reflect a majority of the reads from the V3 and V4 region, using the makeSequenceTable function. We then removed chimeras from the sequence table with the removeBimeraDenova function. The resulting ASVs were then mapped to the known V3 and V4 regions of the isolates in our 35-member SynCom at 98% identity using vsearch's -usearch_global function (2.14.2). We only considered ASVs that mapped to SynCom members in all further 16S analysis.

Analysis of flg22 effect on the assembly of SynCom35. We performed our constrained analysis of principal coordinates (CAPs) similar to Finkel et al. (23). Briefly, the number of reads from ASVs that mapped to each isolate were summed together to reflect a single abundance value for each member of SynCom35. Relative abundances were calculated by dividing each count by the total number of reads mapping to the SynCom35 members in that sample. We performed a constrained analysis of principal coordinates (CAPs) on the root sample's relative abundance data using the capscale function from the vegan version 2.5-6 package in R. We used this function to create a square-rooted Bray-Curtis distance matrix with the vegdist function, and ordinate the matrix based on the model formula: relative_abundance ~ flg22 + experiment_batch. We then performed a PERMANOVA to determine the significance of the model and each of the model terms with 5000 permutations using the anova.cca function from vegan. We used the sum of variance explained calculated from the anova.cca function to determine the constrained and unconstrained variance explained.

Differential abundance of microbes with the addition of flg22 in root samples. We took the raw reads for each bacterial strain and used the DESeq2 version 1.26.0 (24) package in R to call differential abundant microbes between flg22- and mock-treated root samples. We created a DEseq object using the DESeqDataSetfromMatrix function and used the model – reads ~ Biological.Replicate + flg22. To perform the differential abundance analysis, we first estimated the normalization factors using the estimateSizeFactors function implemented in DESeq2 using the poscounts method, which handles bacteria with 0 counts in some of the samples by calculating a modified geometric mean. We then estimated the dispersion estimates for the negative binomial distribution that will be used to call differential abundances with the estimateDispersions function in DESeq2. We then fit coefficients to each microbe indicating the change in abundance between treatments and tested these coefficients for significance using a Wald test implemented in the nbinomWaldTest function in DESeq2. We used an alpha value of 0.05 to assign significance.

Enrichment of members in root or agar samples. Each 16S experiment had a paired root and agar sample. We utilized this design to compare the relative abundance values for each suppressor (SynCom5-S1) and non-suppressor (SynCom-NS1) strain between the root and agar samples. We counted the number of times each strain was found at higher relative abundance values in either the agar or root sample. We did not compare relative abundance values if a strain was absent from both the root and agar samples in an experiment. The maximum number of experiments counted for each strain was 18, the minimum was 0 (for CL18 which was never found in any of our samples), and the median was 18. The counts (we called enrichments) for each strain were combined into the respective SynCom groupings for a total enrichment count of 68 for SynCom5-NS1 and 80 for

SynCom5-S1. The agar and root enrichments were then tabulated (SynCom X enrichment) and a chi-square test was performed on the table with the chisq.test function in R.

Evaluation of the root acute response to flg22. We evaluated the ability of each member of SynCom35 to suppress the roots response to flg22 in the context of an acute exposure to the elicitor (i.e., 5 hours) using the procedures described by Millet et al. (25) (SI Appendix, Fig. S6*D*). For this, we used an Arabidopsis line carrying the *pCYP71A12::GUS* reporter construct, which is activated by flg22 specifically in the root elongation zone (25). Approximately 10 to 15 bleach-sterilized seeds (procedure described above) were inoculated in each well of a 12-well microtiter plate containing 1 mL MS medium (Murashige and Skoog basal medium with vitamins containing 0.5 g/L MES hydrate and 0.5% sucrose at pH 5.7). The plate was kept in a growth chamber under 16-hour light/8-hour dark regime at 21°C day/18°C night for seven days. At the end of the seventh day, the medium was removed with a pipette and replaced by 1 mL MS medium only ('no bacteria' control) or 1 mL MS containing a single bacterial strain at OD_{600nm} of 0.002. The plate was returned to the growth chamber and incubated overnight (~14 hours) to allow bacterial colonization of the roots. The elicitor, flg22, was then added to the medium at a final concentration of 100 nM. Seedlings treated with *Pseudomonas simiae* WCS417 (overnight incubation) or with 10 µM MeJA (added along with flg22) were used as positive controls for the suppression of the flg22 response (25). Plates were kept in the growth chamber for 5 hours after flg22 addition and then submitted to the GUS histochemical assay.

GUS histochemical assays. After the treatment with bacteria and/or flg22, seedlings were washed twice with 50 mM sodium phosphate buffer, pH 7. Then, 1 mL of freshly prepared GUS substrate solution (50 mM sodium phosphate, pH 7; 10 mM EDTA; 0.5 mM $K_4[Fe(CN)_6]$; 0.5 mM $K_3[Fe(CN)_6]$; 0.5 mM X-Gluc; and 0.01% Silwet L-77) was added to each well of the plate, which was subsequently incubated in the dark for 4 hours at 37°C. GUS substrate solution was then replaced by 1 mL of a 3:1 ethanol:acetic acid solution and left at 4°C overnight (~14 hours). Before imaging, this solution was replaced with 1 mL 95% ethanol. Roots were visualized using a Leica M205FA stereoscope coupled to a Leica DFC310FX camera.

Root immune suppression by bacterial culture. We evaluated if culture filtrates of suppressor strains are sufficient to prevent the root response to flg22 following the procedures described by Yu et al. (26) (SI Appendix, Fig. S8*A*). Briefly, Arabidopsis seedlings were surface sterilized and grown for 10 days in a 12-well microtiter plate containing 1 mL MS medium as described above. After this, the plant growth medium was filtered using a 0.22 µM Millipore syringe filter and stored at -20°C until use. Bacteria were grown in 2xYT medium, washed in 10 mM $MgCl_2$ and then inoculated in a 12-well plate containing the plant exudate filtrate at a final OD_{600nm} of 0.002. After

incubating the plate for 22 hours in a growth chamber, cultures were passed through a 0.22 µM Millipore syringe filter, resulting in a bacteria filtrate. This filtrate was then supplied to 10-day-old *pCYP71A12::GUS* Arabidopsis seedlings for 1.5 hours, and 100 nM of flg22 (or a mock control) was then added. After five hours of flg22 treatment, seedlings were submitted to the GUS histochemical assay as described above. Plants growing in the absence of any bacteria or in the culture filtrate of the non-suppressor strain *Ochrobactrum sp*. MF370 were used as controls. The experiment also included *Pseudomonas simiae* strain WCS417, whose acidic culture filtrate suppresses the plant response to flg22 (26). To contrast our suppressor strains to *P. simiae* WCS417, we measured the pH of all bacterial filtrates using an Accumet ab15 pH meter (Fisher Scientific).

Phylogenetic tree construction and annotation. To construct a phylogenetic tree of the 35-member SynCom strains, we trimmed a previously constructed tree (23) that contained a total of 185 strains, including all members of the 35-member SynCom, using the drop.tip function from the ape package version 5.3 in R (27). This phylogenetic tree was based on 47 single copy genes that are present in every isolate of the larger 185-member collection. Single gene alignments were performed using MAFFT (28) and low-quality columns were filtered with trimAl (29). Gene alignments were then concatenated into a single super-alignment and used in the phylogenetic inference using FastTree version 2.1 with the WAG evolution model (30). The resulting tree was annotated with the results from five of our experiments that evaluated the ability of each strain to suppress/activate the plant immune responses: (I) Root-growth inhibition (RGI) triggered by flg22 (Fig. 2*A*); (II) Expression of the flg22 regulon (Fig. 2*B*); (III) Expression of the flg22 core gene set (SI Appendix, Fig. S6*C*); (IV) Interference with the plant response to acute exposure to flg22 (SI Appendix, Fig. S6*D*); (V) Expression of specific sectors of the flg22 regulon (Clusters M3, M4 and M5; Fig. 2*C*).

Quantification of bacterial colonization of plant roots. We evaluated the bacterial levels in plants colonized by communities of suppressor or non-suppressor strains in two independent assays. The first assay (Fig. 3*C*) was based on a community of five suppressors (SynCom5-S1) and five taxonomically matching non-suppressors (SynCom5-NS1). In this experiment, Arabidopsis Col-0 were grown axenically in Johnson medium for seven days (as described above for the SynCom35 experiments) and then transferred to new plates containing either SynCom5-S1 or SynCom5-NS1 (10^5 cells/mL each strain; prepared as described above for SynCom35). Plants transferred to medium without bacteria were used as controls. Plates were kept in a growth chamber under a 9-hour light/15-hour dark regime at 21°C day/18°C night. The root systems of approximately 5 plants per plate were harvested after 12 days for bacteria counting. The experiment was repeated 5 independent times, each with 3 biological replicates per condition. The

second assay (SI Appendix, Fig. S9) utilized a slightly modified community of five suppressors (SynCom5-S2) and five different, not taxonomically matching, non-suppressors (SynCom5-NS2). In this experiment, Arabidopsis Col-0 plants were germinated in 0.5xMS medium in the presence of SynComs ($5x10^5$ cells/mL each strain) or no bacteria and kept in a growth chamber under a 9-hour light/15-hour dark regime at 21°C day/18°C night. The root system of 3-6 seedlings were harvested after 16 days. Strains that comprise all SynComs are listed in SI Appendix, Dataset 1.

To isolate and quantify plant-colonizing bacteria, roots were harvested, rinsed and vortexed vigorously three times with sterile 10 mM $MgCl_2$ to remove agar particles and weakly-associated microbes. Plant material was weighed and then homogenized for 45s in a FastPrep-24 Classic Instrument (MP Biomedicals) in 2 mL tubes containing three 4 mm glass beads and 400 µL 10 mM $MgCl_2$. Homogenized samples were brought to 1 mL by adding 600 µL 10 mM $MgCl_2$, then submitted to a serial dilution. Four microliters of each dilution were inoculated onto LB agar plates (Luria-Bertani; 10g/L tryptone, 5 g/L yeast extract, 5 g/L NaCl and 15 g/L agar). Colony forming units were counted after 1-3 days incubation at 28°C and used to determine the original bacterial abundance per gram of root tissue based on the serial dilution used for counting.

Evaluation of the Arabidopsis transcriptional response to SynComs of suppressors and non-suppressors. We evaluated the transcriptomes of plants grown in the presence of five suppressors (SynCom5-S1) or five taxonomically matching non-suppressors (SynCom5-NS1) (SI Appendix, Fig. S9*B*-*E*). This analysis is part of the experiment described above for the quantification of bacterial growth (shown in Fig. 3*C*). Briefly, seven-day-old Col-0 seedlings were transferred to plates containing no bacteria, SynCom5-S1 or SynCom5-NS1 (10^5 cells/mL each strain; SI Appendix, Dataset 1). No exogenous flg22 was added. Whole seedlings were harvested after twelve days and used for RNA extraction and sequencing as described above. The experiment included six biological replicates per conditions and was repeated two independent times (each with 3 biological replicates). The processing of RNA-seq reads, identification of differentially expressed genes and gene ontology enrichment analyses were performed as described for the other RNA-seq experiments described above. We compared the transcriptomes of plants grown with each SynCom against the 'no bacteria' control using the model: expression ~ SynCom + experiment, where "SynCom" refers to the presence of bacteria (no bacteria, SynCom5-S1 or SynCom5-NS1) and "experiment" refers to each of the two experimental batches. SI Appendix, Dataset 6 presents the metadata information of the experiment, the lists of differentially expressed genes and the complete results of the enrichment analyses.

Evaluation of the growth of commensals in the presence of SynComs. We measured if the root colonization capacity of commensal bacteria (*Ochrobactrum sp.* MF370 or *Pseudomonas*

viridiflava OTU5 p5.e6) is influenced by communities of suppressors (SynCom5-S2) or non-suppressors (SynCom5-NS2) (Fig. 4 and SI Appendix, Dataset 1). For this, approximately 500 Col-0 seeds were sterilized by shaking in 4.25% sodium hypochlorite for 4 min. The sodium hypochlorite was removed, and the seeds were washed four times in sterile water and then resuspended in 0.1% agar. Seeds were vernalized at 4° C for 2-3 days. Seeds were germinated on 0.5X MS medium containing either the suppressor SynCom (SynCom5-S2), the non-suppressor SynCom (SynCom5-NS2) or no bacteria. Plates were kept in a growth chamber under a 9-hour light/15-hour dark regime at 21^{o}C day/18^{o}C night. All bacteria strains were cultured from a single colony and grown in 3 mL of LB medium for 24 h at 28° C and 250 rpm. Cells were centrifuged for 6 min at 4,342 x g and washed three times with 10 mM $MgCl_2$. Media containing SynComs were prepared by embedding each strain at an OD_{600nm} of 0.0005. After two weeks, plants were flooded for 5 min with 7 mL of *Ochrobactrum sp*. MF370 or *Pseudomonas viridiflava* OTU5 strain p5.e6 containing pBBR1MCS-5 at an OD_{600nm} of 0.0001. Seedlings were then transferred to new 0.5X MS agar plates without bacteria. After 30 min, the flooding and transfer step was repeated with the strain in 10 mM $MgCl_2$ containing 0.005% silwet. After 48 h, roots from 3-6 seedlings per replicate were harvested, weighed, and ground for 45 s in a FastPrep-24 Classic Instrument (MP Biomedicals) in a 2 mL microcentrifuge tube containing 400 µL of 10 mM $MgCl_2$ and three 4 mm glass beads (Fisher, Cat. No. 11-312B). Homogenized samples were brought up to 1 mL by adding 600 µL 10 mM $MgCl_2$, then submitted to a serial dilution. Four microliters of each dilution were inoculated onto LB agar plates (Luria-Bertani; 10g/L tryptone, 5 g/L yeast extract, 5 g/L NaCl and 15 g/L agar) containing 25 µg/mL gentamycin or 50 µg/mL kanamycin for antibiotic selection of OTU5 and MF370, respectively. Members of SynCom5-S2 and SynCom5-NS2 were susceptible to these antibiotics. Experiments were performed with three biological replicates and repeated three to four times. All experiments were analyzed together using an ANOVA that controlled for a significant batch effect using the model: log.CFU ~ treatment + batch. We identified truly significant groups with a Tukey test and an alpha of 0.05 using the HSD.test function from the agricolae package in R (31).

Type-3 secretion system deletion in MF79. Two unmarked Type-3 Secretion System (T3SS) deletion mutants of *Dyella japonicum* UNC79MFTsu3.2 (henceforth MF79) were constructed by two-step allelic exchange to test the involvement of the T3SS in suppression of the flg22 response observed by wild-type MF79. The first strain, MF79 Δ*sctUTSR*, has the genes for the inner membrane export apparatus of the T3SS deleted (*sctUTSR,* IMG database gene ID 2558297553-2558297556). The second strain, MF79 ΔT3SS, has a larger deletion comprising the full T3SS (*sctUTSRVCDJLN,* IMG database gene ID 2558297553-2558297569). Knockout vectors pJMC151 and pJMC152 for construction of strains MF79 Δ*sctUTSR* and MF79 ΔT3SS, respectively, were designed based on a genetic system developed for *Burkholderia* spp. and the suicide vector

pMo130 (32). All PCR steps were performed with Q5 High-Fidelity DNA Polymerase (New England Biolabs) including the optional GC enhancer. The pMo130 vector backbone was amplified using primers JMC203-JMC204, cleaned-up, and treated with *DpnI* (New England Biolabs). 800-1000bp regions for homologous recombination flanking genes to be deleted were amplified (pJMC151/152 5': primers JMC403-JMC404, pJMC151 3': primers JMC405-JMC406, pJMC152 3': primers JMC407-JMC408). Vectors pJMC151 and pJMC152 were assembled using HiFi DNA Assembly Mastermix (New England Biolabs), transformed into NEB 5-alpha chemically competent *E. coli* (New England Biolabs) and selected on LB agar with 50 µg/mL kanamycin at 37°C. Plasmid DNA was isolated from clones using the ZR Plasmid Miniprep Classic Kit (Zymo Research) and sequenced by Sanger sequencing. Sequencing-confirmed pJMC151 and pJMC152 were transformed into biparental mating *E. coli* strain WM3064 and selected on LB agar plates containing 50 µg/mL kanamycin and 0.3 mM diaminopimelic acid (DAP) at 37°C.

Biparental mating was performed by growing the bacteria overnight: *Dyella japonicum* MF79 in 2xYT medium at 28°C and *E. coli* WM3064 containing either pJMC151 or pJMC152 in LB with 50 µg/mL kanamycin and 0.3 mM DAP at 37°C. Bacteria were washed three times with 2xYT medium and resuspended in 1/10 of the original volume and mixed in equal proportion donor to recipient and plated on LB agar plates containing 0.3 mM DAP and grown overnight at 28°C. The following day, exconjugants of MF79 were selected by streaking on LB agar plates containing 50 µg/mL kanamycin and lacking DAP and grown at 28°C. Several putative first crossover strains were grown from individual colonies in 2xYT medium containing 50 µg/mL kanamycin and screened using primers outside the regions of homologous recombination (JMC409, JMC410, JMC411) and primers on the pMo130 suicide vector backbone (JMC321, JMC322) to confirm insertion of knockout vectors in the MF79 chromosome at the appropriate location. Positive first crossovers were resolved by passaging the strains once on 2xYT lacking antibiotics, then passaging on media containing 10 g/L tryptone, 5 g/L yeast extract, 100 g/L sucrose, and 1mM IPTG, and finally plating on the same medium containing 1.5% agar. The resulting strains were screened for gene deletion using primers JMC409-JMC410 for strain MF79 Δ*sctUTSR* and primers JMC409-JMC411 for strain MF79 ΔT3SS. Putative positive strains were plate-purified by streaking two additional times on LB agar plates. The gene deletions in the final strains were confirmed again using PCR as described above. Purity of the final deletion strains were confirmed by performing PCR using forward primer JMC409 and reverse primer JMC426 inside the deleted gene *sctU*, which resulted in a 1.2 kb product for wild-type MF79 and no product in the deletion strains. Primers are listed in SI Appendix, Dataset 7 and the confirmatory DNA gel is shown in SI Appendix, Fig. S10*A*. Growth of the knockout mutants was compared to wild-type MF79 by growing the strains in Minimal Medium A (33) with 10 mM sucrose and 0.1% tryptone in an Infinite M200 Pro plate reader (Tecan) at 28°C while measuring OD_{600nm}.

MF79 Transposon insertion library screening. Arabidopsis *pCYP71A12::GUS* seeds were surface sterilized and stratified as described above for 24-48 hours in sterile distilled water, then arrayed in 96-well plates, with 1-3 seeds per well. 80 µL of MS medium was added and seedlings were grown at 16-hour light/8-hour dark regime at 21°C day/18°C night for 7 days.

The RB-TnSeq library for MF79 (34) was plated on LB agar plates containing 50 µg/mL kanamycin and grown at 28°C. Approximately 4500 individual colonies were placed into single wells of 96-deep well plates containing 2xYT medium with 50 µg/mL kanamycin and grown at 28°C. The bacteria were washed 3 times with 10 mM $MgCl_2$, resuspended in MS medium, and then 1 µL was added to each well containing Arabidopsis *pCYP71A12::GUS* seedlings in 80 µL MS. To store the arrayed bacteria, a final concentration of 20% glycerol was added to each well of washed bacteria and the library was frozen at -80ºC. In total, 49 plates were screened comprising approximately 4500 individual transposon insertion strains.

Approximately 16 hours after adding bacteria to the seedlings, 1 µM flg22 peptide was added to the wells. After 5 hours of flg22 treatment, seedlings were submitted to the GUS histochemical assay as described above. Plates were manually inspected for any wells containing plants with blue root tips indicating a failure to suppress the flg22 induction of *pCYP71A12*-driven GUS expression. All putatively positive strains were regrown by streaking from the 96-well plate glycerol stock of the arrayed library to LB plates containing 50 µg/mL kanamycin. Colonies were picked and grown 2xYT medium containing 50 µg/mL kanamycin, washed three times with 10mM $MgCl_2$, and assayed again using the GUS histochemical assay in 48-well plates with 100 nM flg22 peptide to confirm their ability to suppress the flg22 induced GUS expression. In this assay, bacteria were inoculated at an OD_{600nm} of 0.002. Six strains from the mutant library screened in this confirmatory assay were unable to suppress the flg22 induced GUS expression and were subjected to transposon insertion mapping. Growth of the selected Tn mutants were compared to wild-type MF79 by growing the strains in Minimal Medium A (33) with 10 mM sucrose and 0.1% tryptone in an Infinite M200 Pro plate reader (Tecan) at 28°C while measuring $OD600_{nm}$.

Transposon insertion mapping. An arbitrary PCR approach was used to map the transposon insertions in the six strains that lost the ability to suppress the plant response to flg22. PCR steps were performed with Q5 High-Fidelity DNA Polymerase (New England Biolabs) using the optional GC enhancer according to the manufacturer instructions. A first PCR was performed using a transposon kanamycin marker specific primer (JMC525) and arbitrary primer ARB6 (35) with an annealing temperature of 35°C and extension time of 90s for 30 cycles. Following this, a second round of PCR was performed on the product using a primer nested inside the kanamycin resistance gene of the expected product (JMC567) and primer ARB2 (35) with annealing temperature of 71°C

and extension time of 90s for 30 cycles. The resulting PCR product was cleaned up and Sanger sequenced using primer JMC567. BLASTn was used to identify the MF79 genomic sequence adjacent to the transposon insertion and determine the Tn insertion location and, thus, the gene disrupted by the insertion. Primers are listed in SI Appendix, Dataset 7.

Suppression of the flg22 response by *D. japonica* MF79 cell-free supernatant. *D. japonica* MF79 wild-type and the *gspD::Tn* and *gspE::Tn* mutant strains were grown to stationary phase in 2xYT medium. Each strain was washed three times with 10 mM $MgCl_2$ and inoculated at OD_{600nm} of 0.02 into 1xMS medium containing 5 g/L sucrose and 0.1% (w/v) casamino acids (Bacto). Cultures were grown at 21°C with 250 rpm shaking for 18 hours. To remove the bacteria, cultures were centrifuged at 4000 x g for 15 min and the supernatant was filtered through as 0.2 µm filter to prepare cell-free supernatant. To evaluate the potential size of the active suppressive molecule(s), supernatant from the MF79 wild type was passed through a 10,000 MWCO Amicon Ultra-15 spin concentrator (Millipore). The 10 kDa flow-through is the sample that passed through the concentrator. The 10 kDa retentate sample was retained in the concentrator and brought to its original volume with 1xMS medium. Both the 10 kDa retentate and flow-through were sterile filtered prior to use.

pCYP71A12::GUS seedlings were grown in 24-well plates with 500 µL 1xMS medium with sucrose. This growth medium was removed from 7-day-old seedlings and replaced with the sterile cell-free supernatant, 10 kDa retentate, or 10 kDa flow-through samples from MF79 wild-type, *gspD::Tn*, and *gspE::Tn* or a blank medium control. Then, 1 µM flg22 was added to the wells for 5 hours, following which GUS histochemical staining was performed as described above.

Non-suppressor MF370 growth with MF79 10 kDa suppressive fraction. We evaluated if suppression of the flg22 response by *D. japonica* MF79 supernatant enhanced the growth of a non-suppressor commensal strain (Fig. 5*E*). Arabidopsis *pCYP71A12::GUS* seeds were surface sterilized as described above, arrayed in 24-well plates with 5-6 seeds per well, and grown in 500 µL 1xMS medium containing sucrose at 16-hour light/8-hour dark regime at 21°C day/18°C night for 7 days. Then, the wells and seedlings were washed 3 times with 750 µL 0.5x MS lacking sucrose.

Cell-free supernatant from *D. japonica* MF79 wild-type, *gspD::Tn*, and *gspE::Tn* were prepared as described above. To remove sucrose and casamino acids, the cell free supernatant for each was concentrated in a 10,000 MWCO concentrator and exchanged into 0.5xMS lacking sucrose by adding this medium and concentrating three times. The final exchanged 10 kDa retentate was brought to the original volume in 0.5xMS lacking sucrose. 500 µL of 10 kDa retentate exchanged

into 0.5xMS or medium alone as a control was added to the wells of the washed 7-day old seedlings and they were returned to the growth chamber. Approximately 18 hours later, 1 μM flg22 or mock treatment was added to wells for 5 hours. The non-suppressor strain *Ochrobactrum sp.* MF370 was grown to stationary phase in 2xYT medium containing 100 μg/mL ampicillin and washed three times in 10 mM $MgCl_2$. *Ochrobactrum sp.* MF370 was diluted in 0.5xMS and added to the wells at a final OD_{600nm} of 0.0002. Plates were returned to the growth chamber for 2 days. To assess the colonization by *Ochrobactrum sp.* MF370, plants were harvested as described above for the plant colonization competition assay and colony forming units of *Ochrobactrum sp.* MF370 per g plant fresh weight were determined on LB plates containing 100 μg/mL ampicillin.

Statistical information. All statistical tests were performed using R software. All boxplots display the median, 25th and 75th quantiles (box), and the smallest value, largest value, or 1.5*IQR below or above the 25th and 75th quantiles (whiskers). All statistical tests used an alpha value of 0.05 to assign significance unless otherwise stated. When possible, all data points are presented in the figures from all replications performed unless otherwise stated. ANOVAs were performed as a two-way ANOVA to control for experimental biases when analyzing multiple experiments at once. Any time multiple comparisons were made, we corrected our comparisons using a Tukey test. When many statistical tests were performed on the same data and many p-values were obtained we performed Benjamini and Hochberg p-value correction method (FDR) to control for false discovery rate. All statistical analysis methods are described in the figure legends. Code for statistical tests can be found at GitHub (https://github.com/ncolaian/MAE).

Data and code availability. All data generated in this project is publicly available. Raw sequences of 16S amplicon sequencing are available at the NCBI Short Read Archive (SRA) under the accession number PRJNA657936. The metadata file, read count table, relative abundance matrix and DESeq results of this experiment are provided in SI Appendix, Dataset 2. Raw sequences and read count matrices from RNA-seq experiments are available at the NCBI Gene Expression Omnibus (GEO) under the accession number GSE156426. The metadata file, edgeR results, list of heatmap cluster members and raw results from Gene Ontology (GO) enrichment analyses are provided in SI Appendix, Datasets 3 and 4. Scripts used for plotting and data analysis are available at GitHub (https://github.com/ncolaian/MAE).

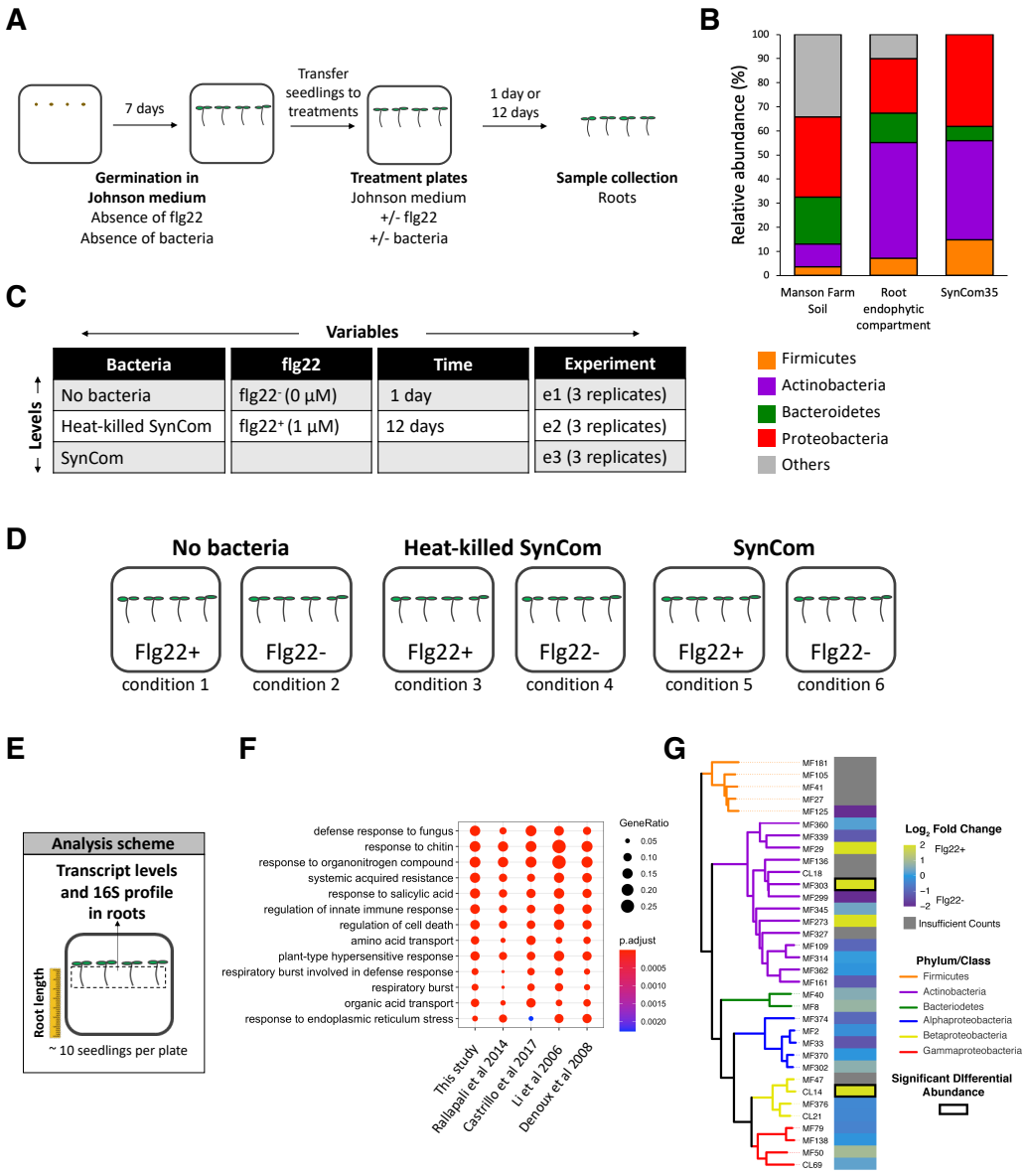

Fig. S1. Evaluating the Arabidopsis root transcriptome and bacterial community in response to the MAMP flg22. (A) Representation of the experimental system used to evaluate the effect of SynCom35 on the root response to flg22. Seeds of wild-type Arabidopsis (Col-0 ecotype) were germinated in Johnson medium under gnotobiotic conditions in the absence of flg22. After seven days, the resulting seedlings were transferred to plates (10 per plate) containing Johnson medium embedded with SynCom35 (10^5 cfu/mL) and/or 1 µM flg22. Roots were harvested for RNA extraction one or twelve days later. (B) Comparison of the bacterial taxonomic composition of Manson Farm soil, the root endophytic compartment of Arabidopsis plants grown in the same soil and of SynCom35. (C) Variables accounted for in the experiment: presence of bacteria, presence of flg22, length of the treatment and experimental batch. (D) A total of six different conditions were evaluated, corresponding to plants treated or not with 1 µM flg22 in the absence of bacteria, with heat-killed SynCom35 or with SynCom35. (E) Cartoon representation of the outputs measured: root length, root transcriptional program (RNA-seq) and root bacterial community profile (16S amplicon sequencing). (F) Seedlings treated with flg22 for 12 days activate defense-related genes in this experimental system. The figure shows biological processes (Gene Ontology) enriched among genes that were up-regulated by flg22 in control plants (in the absence of SynCom35). Four other independent studies are shown for comparison. Note that these other studies are based on plants of different ages, different tissues, different treatment times and flg22 concentration. See SI Appendix, Dataset S5 for details about each experiment. (G) Variation in relative abundance of each member that comprises SynCom35. Only two strains (MF303 and CL14) displayed significant differences in abundance in roots treated with flg22 relative to untreated roots after 12 days.

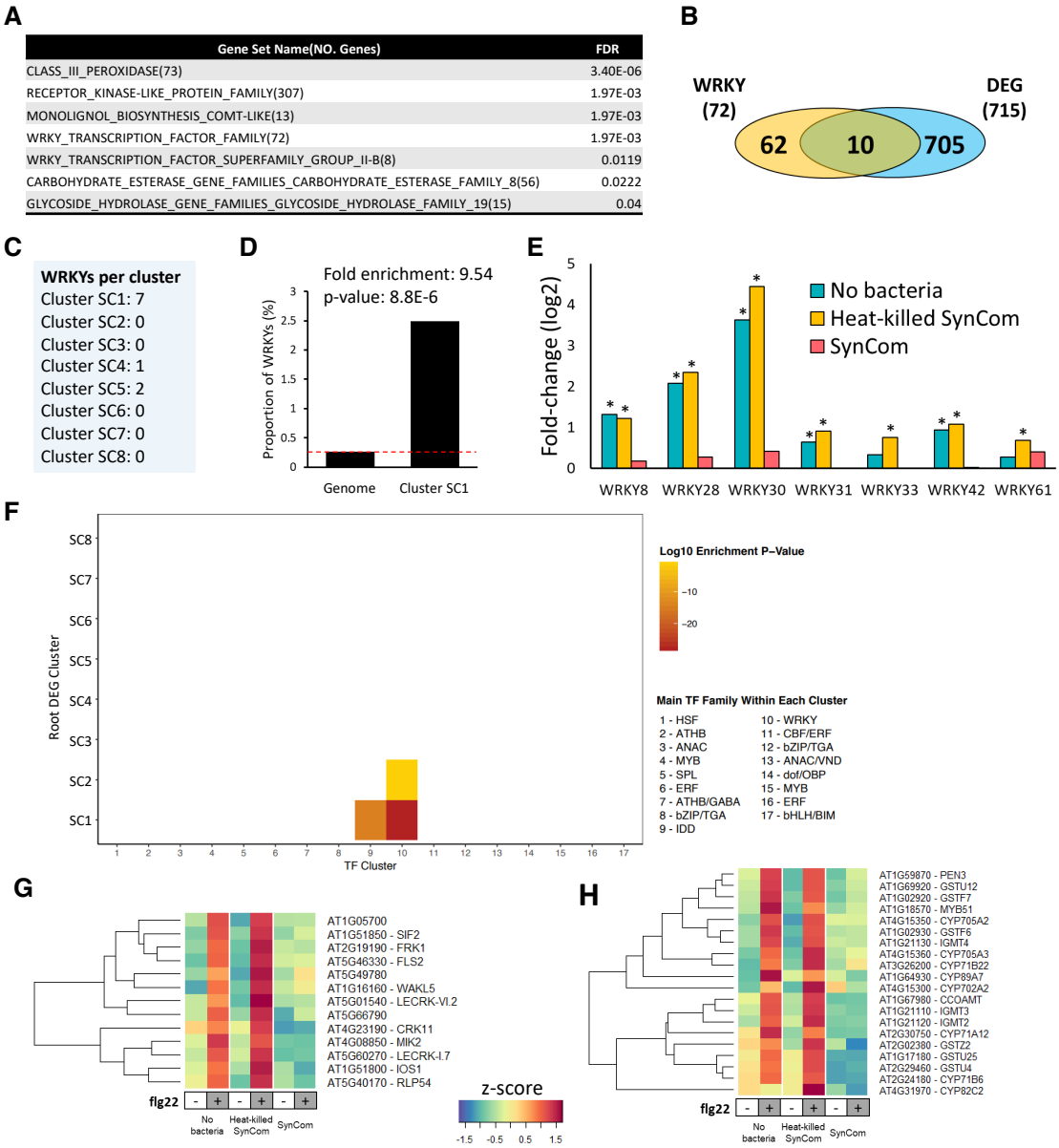

Fig. S2. SynCom35 suppresses key components of the plant immune system. (A) Gene families enriched among the group of flg22-responsive genes that were suppressed by SynCom35 (cluster SC1; Fig. 1*F*). Note the prevalence of defense-related families. (B) A total of 72 genes encoding WRKY transcription factors were annotated in the Arabidopsis Col-0 ecotype at The Arabidopsis Information Resource (TAIR). Among these, 10 were differentially expressed in the roots of plants treated with flg22 in our study. (C) Distribution of *WRKYs* per cluster (Fig. 1*F*). Eight of the ten flg22-responsive *WRKY* genes were up-regulated by flg22 (clusters SC1 and cluster SC4), and two were down-regulated (cluster SC5). Note that seven of the eight *WRKYs* that are activated by flg22 are included in cluster SC1 (i.e., they are suppressed by SynCom35). (D) Enrichment analysis showing that cluster SC1 contains approximately 10 times more *WRKY* genes than expected by chance (hypergeometric test; p-value = 8.8E-6). (E) Fold-changes (flg22 vs mock) of the seven *WRKY* genes included in cluster SC1. Note that these genes are not activated by flg22 when living SynCom35 is also present. Asterisks indicate genes that are differentially expressed based on the edgeR analysis. (F) Genes containing WRKY-binding motifs in their promoters (i.e., putative WRKY targets) are highly enriched in cluster SC1 and, to a lesser extent, in cluster SC2. (G) Expression profile of receptor kinase-like genes found in cluster SC1 (Fig. 1*F*). FRK1 is a widely used as a marker of MTI and FLS2 is the flg22 receptor. (H) Expression profile of genes involved in the synthesis of secondary metabolites found in cluster SC1 (Fig. 1*F*).

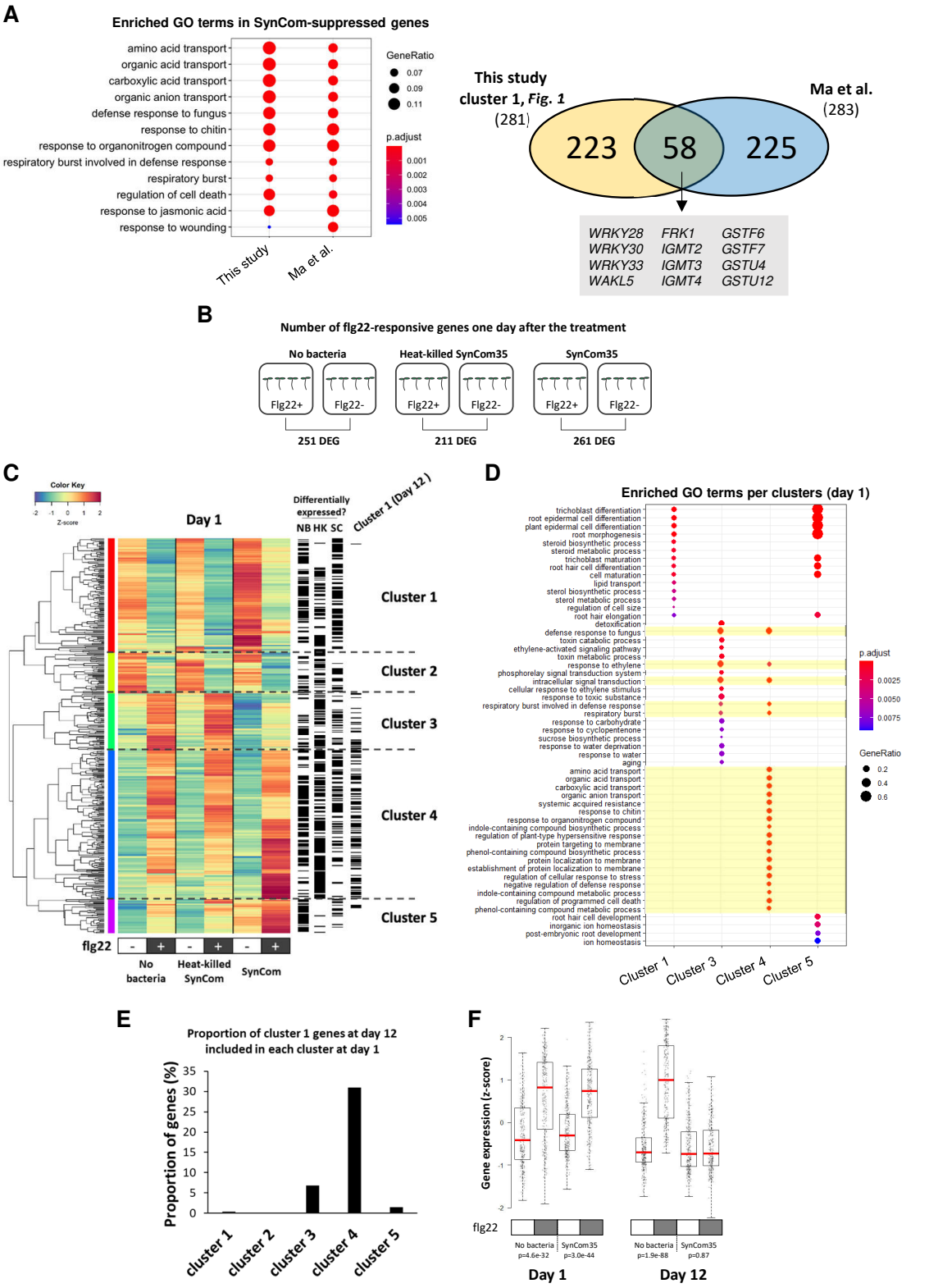

Fig. S3. SynCom35 actively suppresses an ongoing immune response that is also observed in other plant-microbiota interactions. (A) Suppression of defense-related genes is also observed with an independently derived SynCom (Ma et al., 2020). The left side shows that the genes suppressed by the SynCom reported by Ma et al. are enriched in the same biological processes identified in the genes suppressed by SynCom35 in this study (cluster SC1, Fig. 1*F*). p-values were adjusted with the FDR method.

The right side shows the overlap between the two sets of genes, highlighting 58 genes that are commonly suppressed by the SynComs in these independent studies (p=2.53E-58; hypergeometric test). Representative shared genes are shown in the grey box. The complete list of shared genes is shown in SI Appendix, Dataset S3. (B) Number of differentially expressed genes one day after the treatment of roots with flg22 (or mock) in the absence of bacteria, with heat-killed SynCom35 or with SynCom35 alive. (C) Hierarchical clustering of the 449 genes that responded to flg22 in at least one of the experimental conditions one day after treatment. In contrast to the results observed 12 days after treatment (Fig. 1*F*), SynCom35 does not cause a major interference in the root response to flg22 at day 1, indicating that SynCom35 interferes with an ongoing immune response. Indeed, flg22-responsive genes that are suppressed by SynCom35 at day 12 (Cluster 1, Fig. 1*F*) are activated at day 1 (black marks in the "Cluster 1" lane on the right of the heatmap). Genes that respond to flg22 significantly in each of the treatments at day 1 according to edgeR are indicated with black marks on the right in the "Differentially expressed" lanes (NB: no bacteria; HK: heat-killed SynCom35; SC: SynCom35). (D) Gene ontology enrichment analyses showing enriched biological processes in each of the five clusters. Cluster 4, which contains defense-related genes, is highlighted in yellow. No biological processes were enriched in Cluster 2. p-values were adjusted with the FDR method. (E) Proportion of SynCom35-suppressed genes at day 12 (Cluster 1; Fig. 1*F*) that is present in each cluster at day 1. Note that over 30% of the genes suppressed by SynCom35 at day 12 are included in Cluster 4 at day 1. (F) Expression profile of the 281 flg22-responsive genes that are suppressed by SynCom35 at day 12 (Cluster SC1; Fig. 1*F*). Note that the expression of these genes is increased by flg22 in the absence of bacteria at both time points (1 and 12 days after treatment). However, their expression is reduced in the presence of SynCom35 only 12 days after treatment. The p-values on the bottom refer to the comparison between groups (flg22 vs mock) for each condition using t-tests.

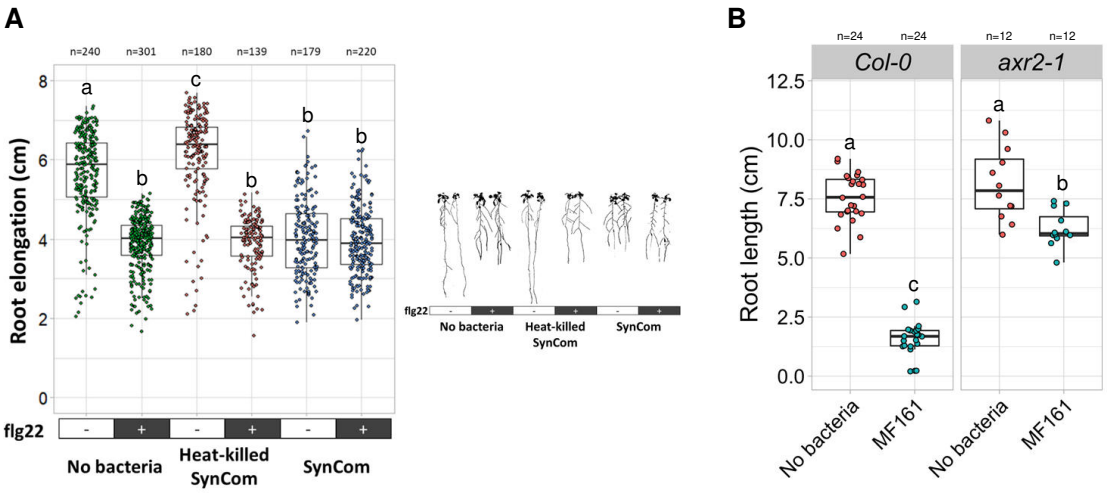

Fig. S4. SynCom35 effects on the Arabidopsis root morphology. (A) Root elongation measured in Arabidopsis seedlings grown in the absence of bacteria, with heat-killed SynCom35 and with SynCom35. For each of these three conditions, plants were exposed or not to 1 µM flg22, resulting in six treatments. Root growth inhibition (RGI) was induced by flg22 in plants grown in the absence of bacteria or with heat-killed SynCom35. Seedlings grown with SynCom35 displayed shorter roots even in the absence of flg22. Multiple comparisons were performed with ANOVA followed by a Tukey test (α = 0.05). Representative images of seedlings from each treatment are shown on the right. (B) The auxin-producing strain *Arthrobacter sp*. MF161 included in SynCom35 induces the RGI phenotype when in mono-association with Arabidopsis. This phenotype is significantly reduced in the auxin-resistant mutant line *axr2-1* suggesting that it is mediated by an auxin response. Multiple comparisons were performed with ANOVA followed by a Tukey test (α = 0.05).

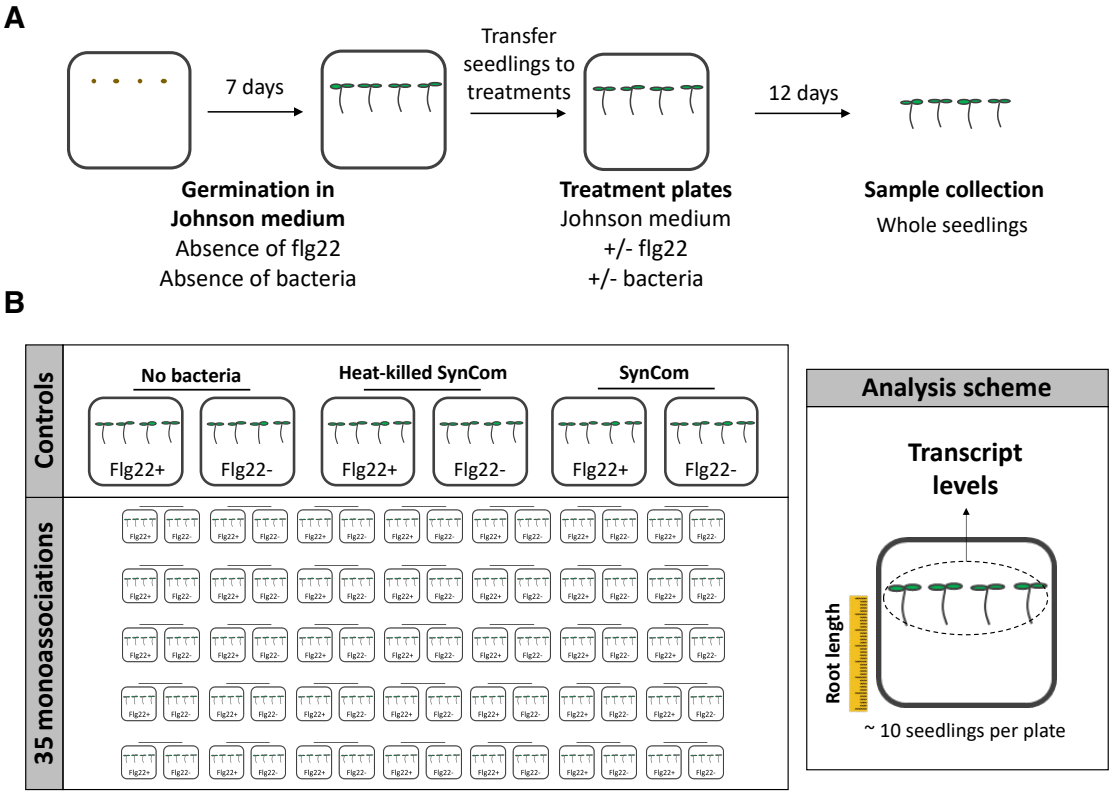

Fig. S5. Design of the mono-association experiment. (A) Representation of the experimental system used to evaluate the effect of each of the 35 members of SynCom35 on Arabidopsis seedlings. Seeds of wild-type Arabidopsis (Col-0 ecotype) were germinated in Johnson medium under gnotobiotic conditions in the absence of flg22. After seven days, the resulting seedlings were transferred to plates (10 per plate) containing Johnson medium embedded with a single bacterial strain (10^5 cfu/mL) in the presence or not of 1 µM flg22. Whole seedlings were harvested for RNA extraction twelve days later. Plants grown in the absence of bacteria and with heat-killed SynCom35 and SynCom35 were used as controls. (B) Representation of the conditions included in the experiment. A total of 76 different conditions were evaluated (35 strains and 3 controls x 2 treatments) in three independent experiments, each containing 3 biological replicates (total of 9 biological replicates per condition). The root length and the plant transcriptional program (RNA-seq) was assessed in each sample.

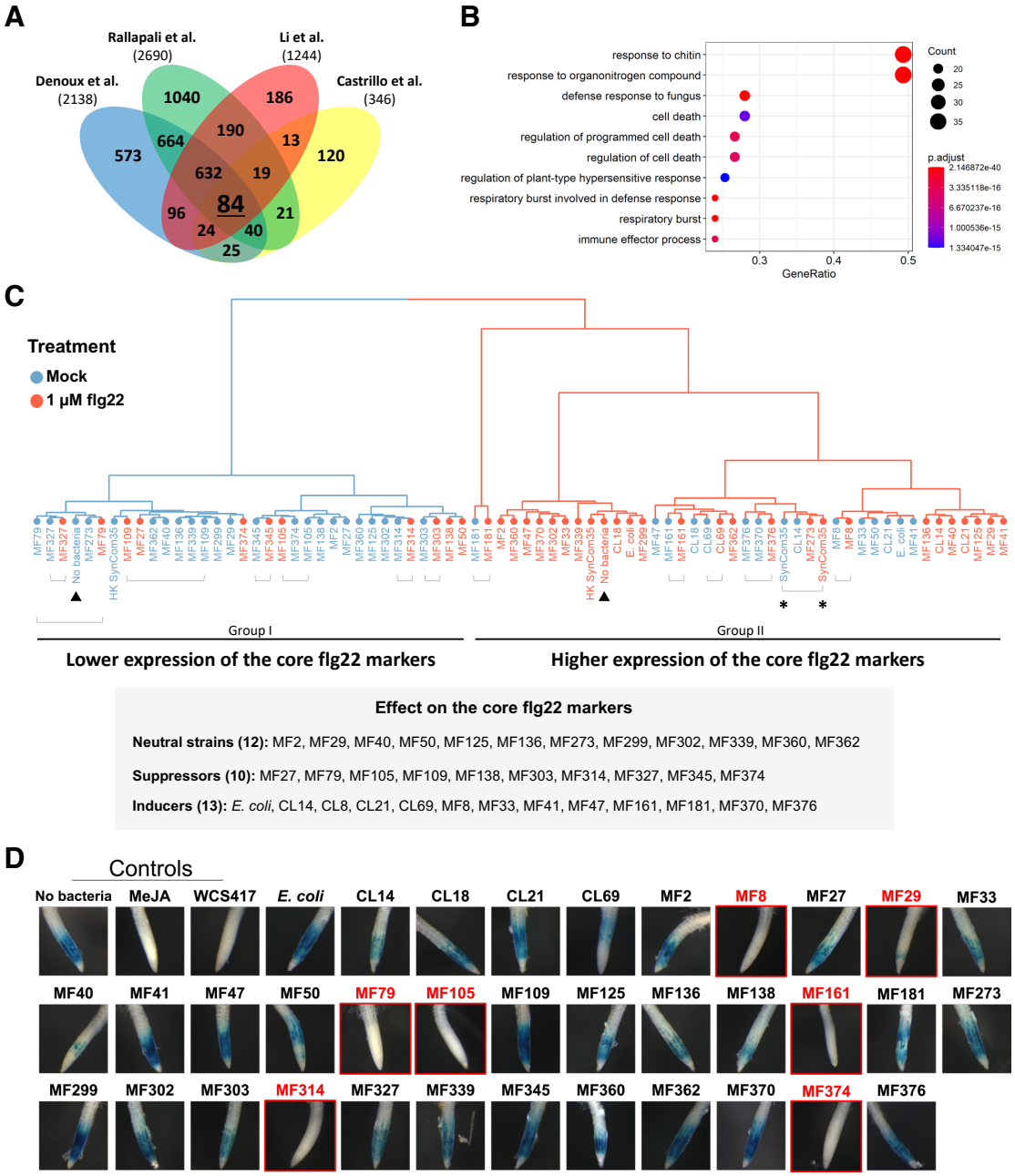

Fig. S6. Members of SynCom35 interfere with the expression of a robust set of 84 core flg22-responsive genes in a chronic treatment and also suppress the plant acute response to the elicitor. (A) Venn diagram with the overlap among genes found up-regulated by flg22 in four different gene expression experiments (1, 38–40). The intersection (84 genes; SI Appendix, Dataset 5) was used as a robust marker set of the flg22 response. (B) A Gene Ontology enrichment analysis showed that this core set of genes is highly enriched in immunity-related biological processes. p-values were adjusted with the FDR method. (C) Plants grown in mono-association with SynCom35 members were clustered based on the expression of the 84 markers genes of the flg22 response (core flg22 markers). Plants grown with SynCom35 (asterisks), heat-killed SynCom35 and in the absence of any bacteria ("no bacteria"; triangles) were also included in the experiment. For each condition, plants were exposed to 1 µM flg22 (red labels) or a mock treatment (blue labels). Note that samples are organized in two main clusters: the cluster on the left includes most of the mock-treated plants (blue) and displays lower expression of the core flg22 marker set. The cluster on the right includes most of the flg22-treated plants (red) and displays higher expression of the same marker set. In the presence of some strains, plants treated with flg22 (red) displayed low expression of the flg22 response marker set and, thus, grouped with mock-treated samples on the left. These were considered suppressor strains. In

other cases, bacteria triggered higher expression of the flg22 marker set even in the absence of exogenous MAMP (blue), grouping with flg22-treated plants on the right. These were considered inducer strains. Lines under the labels connect plants treated with a specific strain for which addition of flg22 had no major effect on the expression of the 84 marker genes (i.e., mock- and flg22-treatments grouped together). The chart below lists strains with neutral, suppressive or inducive effect on the flg22 markers. (D) At least seven members of SynCom35 (labeled in red) suppress the acute flg22 response in Arabidopsis roots. The reporter line carrying the *pCY71A12::GUS* construct (25) was grown for seven days in gnotobiotic conditions and then inoculated with each single strain individually at a final OD of 0.002. After 14h of co-cultivation, plants were treated with 100 nM flg22 for 5h. A blue signal in the elongation zone indicates that the *pCYP71A12* was activated by flg22. MeJA and *Pseudomonas simiae* WCS417 were previously shown to suppress MTI in the roots and were used as controls in the experiment (25). The experiment was performed at least two independent times for each strain. Each time included 2 repetitions (wells) consisting of approximately 10 seedlings each.

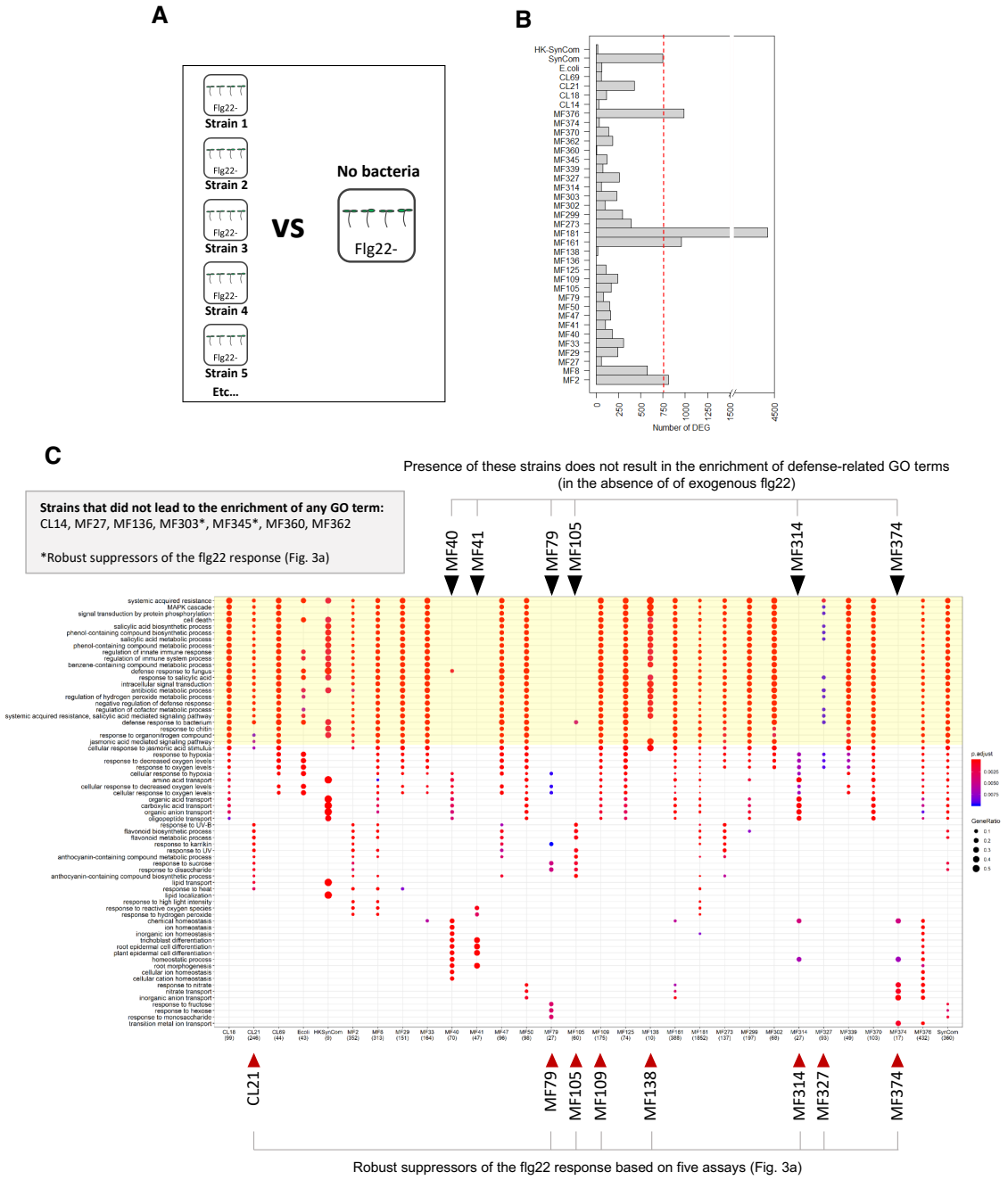

Fig. S7. Most, but not all, members of SynCom35 trigger the activation of plant defense genes to some extent when in mono-association. (A) Representation of the comparisons performed to evaluate the effect that each member of SynCom35 has on the plant. The transcriptome of plants grown with individual strains in the absence of flg22 was compared to the control condition (no addition of bacteria or flg22). (B) Number of differentially expressed genes identified in plants grown with each SynCom35 member. The red line depicts the number of differentially expressed genes identified in plants grown in the presence of SynCom35. (C) Gene Ontology (GO) enrichment analysis showing biological processes enriched in the sets of genes up-regulated by each strain. The area shaded in yellow corresponds to GO terms related to immune responses. Note that most strains trigger a transcriptional program that is enriched in defense-related genes. The six strains indicated with arrows on the top (MF40, MF41, MF79, MF105, MF314 and MF374) do not lead to the activation of the plant immune response but trigger the activation of other biological processes. Seven other strains (MF27, MF136, MF303, MF345, MF360, MF362 and CL14) did not result in the enrichment of GO processes and are not shown in the figure. Strains defined as robust suppressors (Fig. 3*A*) are labeled on the bottom. p-values were adjusted with the FDR method.

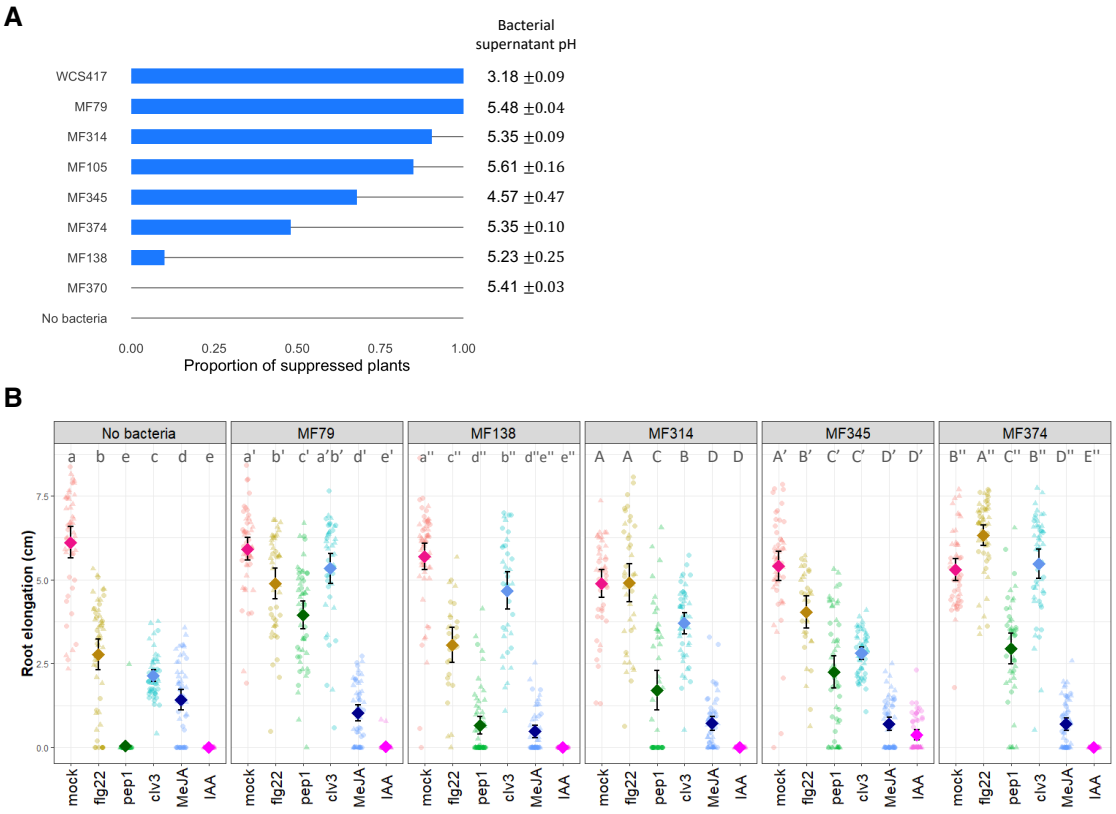

Fig. S8. Suppression of the plant immune system by commensal bacteria likely occurs through multiple different mechanisms. (A) Six robust suppressor strains were evaluated for their ability to prevent the root response to flg22 through acidification of the extracellular medium. The assay was performed as described by Yu et al. (2019) using cell-free bacterial supernatants and the Arabidopsis *pCYP71A12::GUS* reporter line. *Pseudomonas simiae* WCS417, which suppresses the flg22 response through medium acidification, was used as a positive control. The non-suppressor strain *Ochrobactrum sp.* MF370 was used as a negative control. The bars show the proportion of plants that did not respond to flg22 in each treatment (i.e., proportion of suppressed plants). A total of 20-25 seedlings were evaluated in the treatment of each suppressor strain. Note that the cell-free supernatant of most strains was sufficient to suppress the root response to flg22. Consistent with previous observations (Yu et al., 2019), *P. simiae* WCS417 lowered the extracellular pH to ~3. However, the supernatant of our suppressor strains remained at pH of 5-6, which is sufficient for a normal response to flg22 (Yu et al., 2019). This indicates that these strains do not employ the acidification of the extracellular medium as a strategy to suppress MTI. (B) Evaluation of the ability of suppressor strains to interfere with the root growth inhibition (RGI) phenotype induced by various molecules. The peptides flg22 (1 µM), pep1 (1 µM) and clv3 (1 µM) as well as the hormones methyl jasmonate (MeJA; 10 µM) and indole-3-acetic acid (IAA; 1 µM) were used. Seven-day-old Col-0 seedlings were transferred to Johnson medium embedded with bacteria (OD_{600nm}=0.0001) and the molecules of interest and grown at 9h light/15h dark (21°C light/18°C dark). Root elongation was Note that all molecules induce RGI in plants grown in the absence of bacteria (control treatment). measured after 12 days. Most strains suppress the RGI phenotype caused by peptides but not by the two hormones. Diamonds represent means with two times standard error. Multiple comparisons within each 'bacteria' condition were performed with ANOVA followed by a Tukey test (letters on the top).

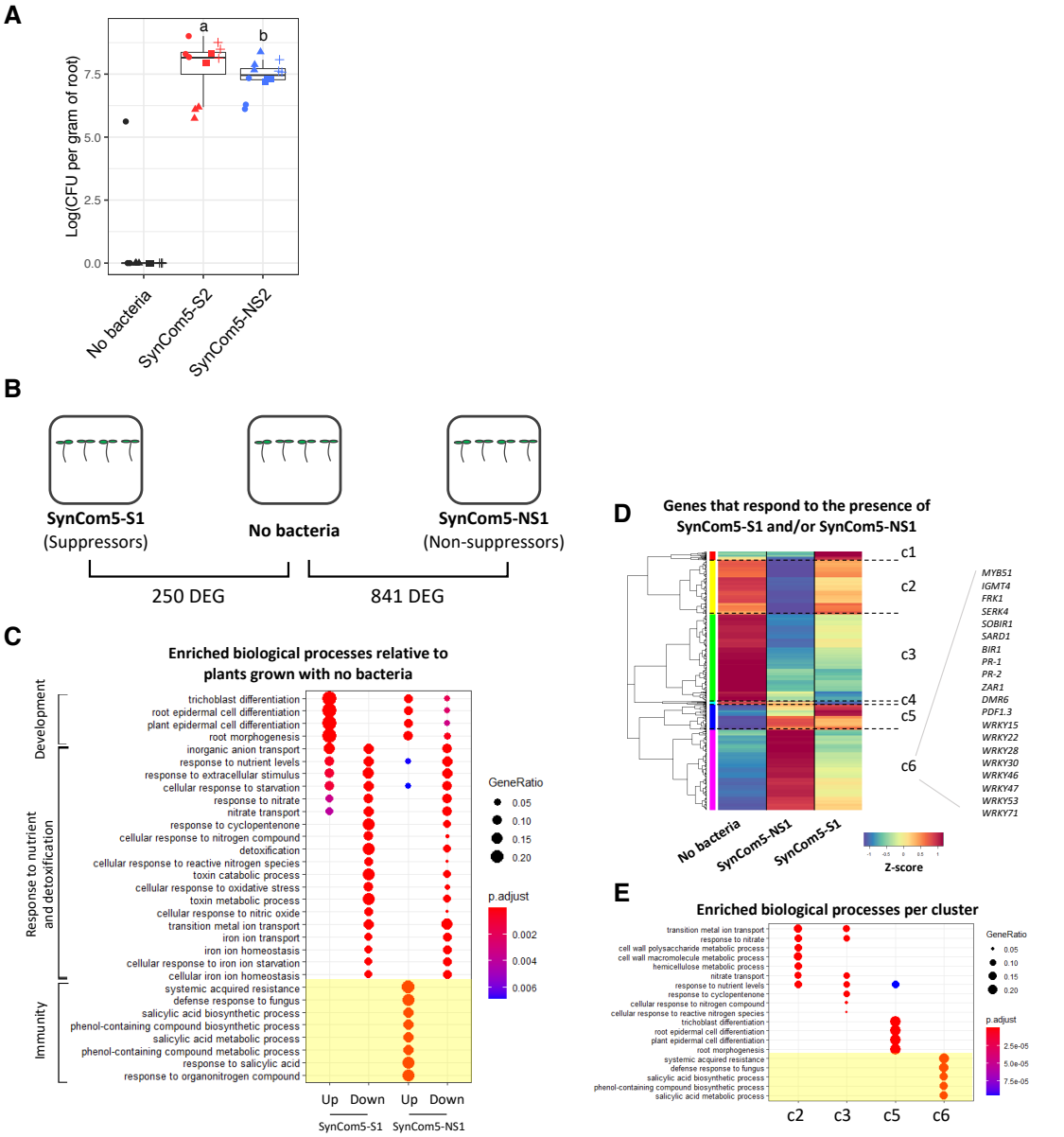

Fig. S9. A community of non-suppressor bacteria triggers defense responses in Arabidopsis. (A) Evaluation of bacteria colonization of Arabidopsis roots. A SynCom made of five suppressors (SynCom5-S2) grows to higher levels in the roots than a SynCom made of five non-suppressors (SynCom5-NS2). The experiment was performed four independent times, each with three biological replicates per condition (n=12). Different symbols represent different experimental repetitions. This experiment complements the results presented in Fig. 3*C* and was performed in a different experimental system (see methods) using different SynComs. (B) Transcriptional analysis of plants grown in the absence of bacteria or with communities of suppressors (SynCom5-S1) and non-suppressor (SynCom5-NS1) strains. The number of differentially expressed genes (DEG) is shown under each comparison. No exogenous flg22 was added. (C) Gene ontology enrichment analysis showing biological processes enriched in the sets of genes up- or down-regulated in plants grown with SynCom5-S1 or SynCom5-NS1 relative to axenic conditions. Note the absence of immunity-related terms in plants colonized with SynCom5-S1 (shaded in yellow). (D) Hierarchical clustering of 925 genes that responded to SynCom5-S1, SynCom5-NS1 or both. Six clusters were defined. Example of defense-related genes are shown on the right. (E) Gene ontology enrichment analysis of each cluster defined in panel (D). Note that immunity-related terms are enriched in cluster c6, which includes genes more expressed in the presence of SynCom5-NS1. Clusters c1 and c4 do not have enriched terms. SI Appendix, Dataset 6 presents metadata information of the experiment, the lists of differentially expressed genes and the complete results of the enrichment analyses.

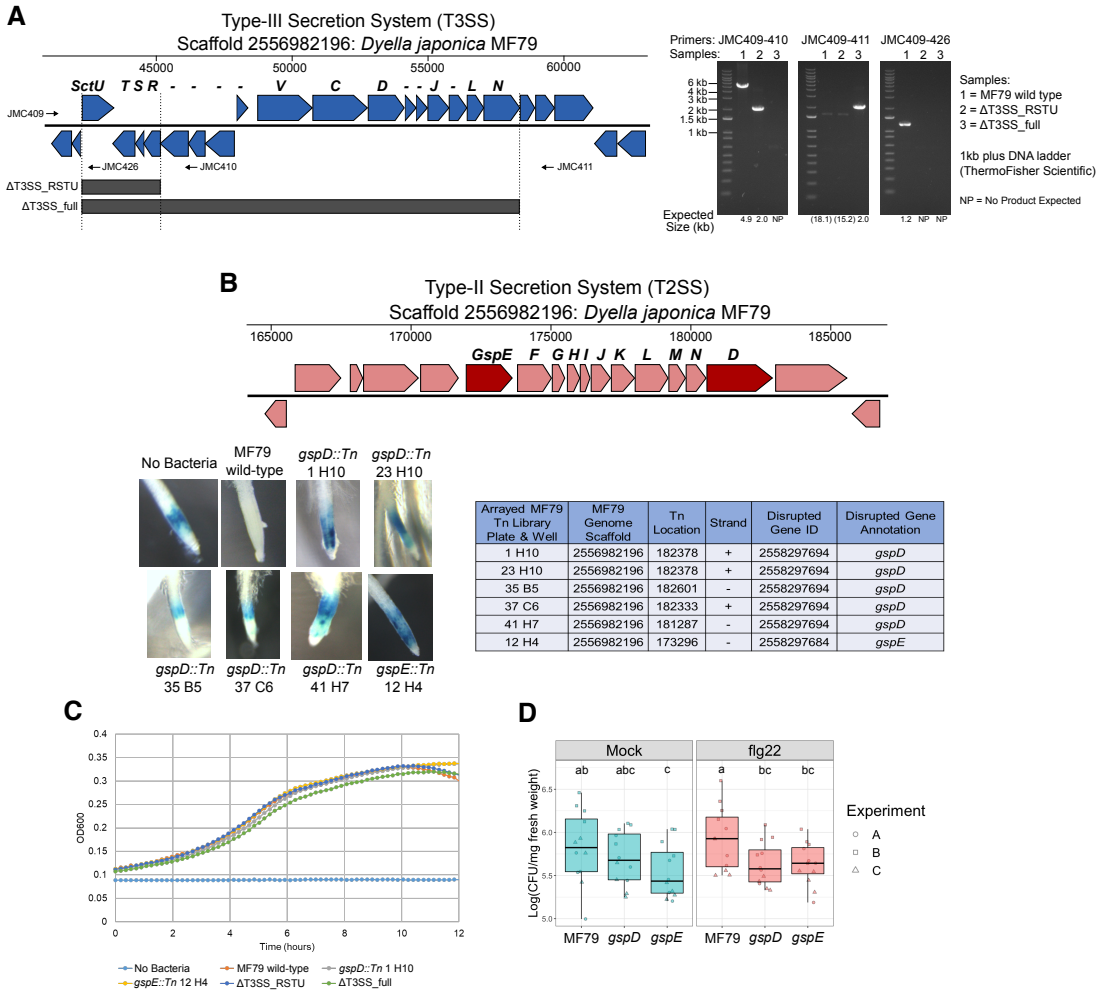

Arrayed MF79 Tn Library Plate & Well	MF79 Genome Scaffold	Tn Location	Strand	Disrupted Gene ID	Disrupted Gene Annotation
1 H10	2556982196	182378	+	2558297694	*gspD*
23 H10	2556982196	182378	+	2558297694	*gspD*
35 B5	2556982196	182601	-	2558297694	*gspD*
37 C6	2556982196	182333	+	2558297694	*gspD*
41 H7	2556982196	181287	-	2558297694	*gspD*
12 H4	2556982196	173296	-	2558297684	*gspE*

Fig. S10. The T2SS and not the T3SS of *Dyella japonica* MF79 is required for suppression of the flg22 response. (A) Gene map for the *Dyella japonica* MF79 type-III secretion system (T3SS, *Sct* genes). DNA coordinates on Scaffold 2556982196 are identified above the map. Genes deleted in the MF79 ΔT3SS_RSTU and MF79 ΔT3SS_full mutants are marked below the map. DNA gels confirming gene knockouts and strain purity in these mutants are shown to the right. Expected product sizes are shown below the gels. The location of primers used to screen these mutants are marked in the T3SS map. Primers sequences are available in SI Appendix, Dataset 7. (B) Gene map for the *Dyella japonica* MF79 type-II secretion system (T2SS, *Gsp* genes). Six strains with loss of flg22-response suppression were identified from the arrayed MF79 transposon insertion library. Transposon insertion locations were identified by arbitrary PCR. At left, GUS expression assay demonstrating loss of flg22-response suppression by the 6 strains (5 insertions in *GspD*, 1 insertion in *GspE*). Genes disrupted in the MF79 *gspE::Tn* and *gspD::Tn* strains are highlighted in dark red in the map of the T2SS. (C) Growth of the MF79 wild-type, T3SS deletion, and T2SS transposon insertion mutant strains in Minimal Medium A with 10 mM sucrose and 0.1% tryptone. (D) The ability to suppress the plant immune system correlates with enhanced colonization of Arabidopsis roots. Although *gspD* and *gspE* mutants did not display impaired growth *in vitro*, they are poorer colonizers of Arabidopsis roots than the wild-type strain. Plants were cultivated with each strain in mono-colonization for 5 days in the presence (red) or not (blue) of 1 μM flg22.

Dataset S1 (separate file). Bacterial strains used in this study.
Spreadsheet with detailed information about the bacteria used in the experiments and the composition of each SynCom constructed. The 16S sequence of each strain is also provided.

Dataset S2 (separate file). 16S amplicon sequencing.
Spreadsheet with information about the sequencing of SynCom 16S amplicons. The file contains the metadata of the experiment, raw counts, relative abundance and the results of the differential abundance analysis.

Dataset S3 (separate file). SynCom35 RNA-seq experiment.
Spreadsheet with information about the RNA-seq experiment of plants exposed to SynCom35 and flg22. The file contains the metadata of the experiment, the results of differential expression analyses, a list of members in each heatmap cluster and Gene Ontology enrichment analyses.

Dataset S4 (separate file). Mono-associations RNA-seq experiment.
Spreadsheet with information about the RNA-seq experiment of plants exposed to individual bacteria and flg22. The file contains the metadata of the experiment, the results of differential expression analyses, a list of members in each heatmap cluster and Gene Ontology enrichment analyses.

Dataset S5 (separate file). Marker genes of the flg22 response.
Spreadsheet with a set of literature-curated genes that were up-regulated by flg22 in four independent studies.

Dataset S6 (separate file). SynCom5-S1 and SynCom5-NS1 RNA-seq experiment.
Spreadsheet with information about the RNA-seq experiment of plants exposed to SynCom5-S1 (suppressors) and SynCom5-NS1 (non-suppressors). The file contains the metadata of the experiment, the results of differential expression analyses, a list of members in each heatmap cluster and Gene Ontology enrichment analyses.

Dataset S7 (separate file). Genetic analyses of *Dyella japonica* MF79
Spreadsheet with primers used for the generation of T3SS knockout strains and for transposon mapping. Detailed information about the non-suppressing mutants identified in the RB-TnSeq library is also provided.

SI References

1. G. Castrillo, *et al.*, Root microbiota drive direct integration of phosphate stress and immunity. *Nature* **543**, 513–518 (2017).

2. C. A. Schneider, W. S. Rasband, K. W. Eliceiri, NIH Image to ImageJ: 25 years of image analysis. *Nat. Methods* **9**, 671–675 (2012).

3. H. Wickham, *ggplot2: elegant graphics for data analysis* (springer, 2016).

4. Z. Gu, R. Eils, M. Schlesner, Complex heatmaps reveal patterns and correlations in multidimensional genomic data. *Bioinformatics* **32**, 2847–2849 (2016).

5. S. S. Abby, B. Néron, H. Ménager, M. Touchon, E. P. C. Rocha, MacSyFinder: a program to mine genomes for molecular systems with an application to CRISPR-Cas systems. *PLoS ONE* **9**, e110726 (2014).

6. J. Logemann, J. Schell, L. Willmitzer, Improved method for the isolation of RNA from plant tissues. *Anal. Biochem.* **163**, 16–20 (1987).

7. A. M. Bolger, M. Lohse, B. Usadel, Trimmomatic: a flexible trimmer for Illumina sequence data. *Bioinformatics* **30**, 2114–2120 (2014).

8. D. Kim, B. Langmead, S. L. Salzberg, HISAT: a fast spliced aligner with low memory requirements. *Nat. Methods* **12**, 357–360 (2015).

9. Y. Liao, G. K. Smyth, W. Shi, The Subread aligner: fast, accurate and scalable read mapping by seed-and-vote. *Nucleic Acids Res.* **41**, e108 (2013).

10. P. Ewels, M. Magnusson, S. Lundin, M. Käller, MultiQC: summarize analysis results for multiple tools and samples in a single report. *Bioinformatics* **32**, 3047–3048 (2016).

11. D. J. McCarthy, Y. Chen, G. K. Smyth, Differential expression analysis of multifactor RNA-Seq experiments with respect to biological variation. *Nucleic Acids Res.* **40**, 4288–4297 (2012).

12. M. D. Robinson, D. J. McCarthy, G. K. Smyth, edgeR: a Bioconductor package for differential expression analysis of digital gene expression data. *Bioinformatics* **26**, 139–140 (2010).

13. M. D. Robinson, A. Oshlack, A scaling normalization method for differential expression analysis of RNA-seq data. *Genome Biol.* **11**, R25 (2010).

14. Y. Benjamini, Y. Hochberg, Controlling the false discovery rate: a practical and powerful approach to multiple testing. *Journal of the Royal statistical society: series B (Methodological)* **57**, 289–300 (1995).

15. H. Heberle, G. V. Meirelles, F. R. da Silva, G. P. Telles, R. Minghim, InteractiVenn: a web-based tool for the analysis of sets through Venn diagrams. *BMC Bioinformatics* **16**, 169 (2015).

16. T. Wei, V. Simko, *R package "corrplot": Visualization of a Correlation Matrix* (2017).

17. J. Oksanen, *et al.*, *vegan: Community Ecology Package* (2019).

18. G. R. Warnes, *et al.*, *gplots: Various R Programming Tools for Plotting Data* (2020).

19. G. Yu, L.-G. Wang, Y. Han, Q.-Y. He, clusterProfiler: an R package for comparing biological themes among gene clusters. *OMICS* **16**, 284–287 (2012).

20. X. Yi, Z. Du, Z. Su, PlantGSEA: a gene set enrichment analysis toolkit for plant community. *Nucleic Acids Res.* **41**, W98-103 (2013).

21. S. Herrera-Paredes, *AMOR: Abundance Matrix Operations in R* (2018).

22. B. J. Callahan, *et al.*, DADA2: High-resolution sample inference from Illumina amplicon data. *Nat. Methods* **13**, 581–583 (2016).

23. O. M. Finkel, *et al.*, A single bacterial genus maintains root growth in a complex microbiome. *Nature* (2020) https:/doi.org/10.1038/s41586-020-2778-7.

24. M. I. Love, W. Huber, S. Anders, Moderated estimation of fold change and dispersion for RNA-seq data with DESeq2. *Genome Biol.* **15**, 550 (2014).

25. Y. A. Millet, *et al.*, Innate immune responses activated in Arabidopsis roots by microbe-associated molecular patterns. *Plant Cell* **22**, 973–990 (2010).

26. K. Yu, *et al.*, Rhizosphere-Associated *Pseudomonas* Suppress Local Root Immune Responses by Gluconic Acid-Mediated Lowering of Environmental pH. *Current Biology* **29**, 3913-3920.e4 (2019).

27. E. Paradis, K. Schliep, ape 5.0: an environment for modern phylogenetics and evolutionary analyses in R. *Bioinformatics* **35**, 526–528 (2019).

28. K. Katoh, D. M. Standley, MAFFT multiple sequence alignment software version 7: improvements in performance and usability. *Mol. Biol. Evol.* **30**, 772–780 (2013).

29. S. Capella-Gutiérrez, J. M. Silla-Martínez, T. Gabaldón, trimAl: a tool for automated alignment trimming in large-scale phylogenetic analyses. *Bioinformatics* **25**, 1972–1973 (2009).

30. M. N. Price, P. S. Dehal, A. P. Arkin, FastTree 2--approximately maximum-likelihood trees for large alignments. *PLoS ONE* **5**, e9490 (2010).

31. F. de Mendiburu, *agricolae: Statistical Procedures for Agricultural Research* (2020).

32. M. A. Hamad, S. L. Zajdowicz, R. K. Holmes, M. I. Voskuil, An allelic exchange system for compliant genetic manipulation of the select agents *Burkholderia pseudomallei* and *Burkholderia mallei*. *Gene* **430**, 123–131 (2009).

33. F. Ausubel, *et al.*, *Current Protocols in Molecular Biology* (Wiley Interscience, New York, 1996).

34. M. N. Price, *et al.*, Mutant phenotypes for thousands of bacterial genes of unknown function. *Nature* **557**, 503–509 (2018).

35. G. A. O'Toole, *et al.*, Genetic approaches to study of biofilms. *Meth. Enzymol.* **310**, 91–109 (1999).

36. D. S. Lundberg, *et al.*, Defining the core Arabidopsis thaliana root microbiome. *Nature* **488**, 86–90 (2012).

37. K.-W. Ma, *et al.*, Coordination of microbe-host homeostasis via a crosstalk with plant innate immunity. *Research Square (pre-print)* (2020).

38. C. Denoux, *et al.*, Activation of defense response pathways by OGs and Flg22 elicitors in Arabidopsis seedlings. *Mol Plant* **1**, 423–445 (2008).

39. G. Rallapalli, *et al.*, EXPRSS: an Illumina based high-throughput expression-profiling method to reveal transcriptional dynamics. *BMC Genomics* **15**, 341 (2014).

40. B. Li, *et al.*, Phosphorylation of trihelix transcriptional repressor ASR3 by MAP KINASE4 negatively regulates Arabidopsis immunity. *Plant Cell* **27**, 839–856 (2015).